

Implicit Diffusion: Efficient Optimization through Stochastic Sampling

Pierre Marion^{1*} Anna Korba² Peter Bartlett³ Mathieu Blondel³ Valentin De Bortoli³ Arnaud Doucet³
Felipe Llinares-López[†] Courtney Paquette³ Quentin Berthet³

Abstract

We present a new algorithm to optimize distributions defined implicitly by parameterized stochastic diffusions. Doing so allows us to modify the outcome distribution of sampling processes by optimizing over their parameters. We introduce a general framework for first-order optimization of these processes, that performs jointly, in a single loop, optimization and sampling steps. This approach is inspired by recent advances in bilevel optimization and automatic implicit differentiation, leveraging the point of view of sampling as optimization over the space of probability distributions. We provide theoretical guarantees on the performance of our method, as well as experimental results demonstrating its effectiveness in real-world settings.

1. Introduction

Sampling from a target distribution is a ubiquitous task at the heart of various methods in machine learning, optimization, and statistics. Increasingly, sampling algorithms rely on iteratively applying large-scale parameterized functions (e.g. neural networks with trainable weights) to samples, such as in denoising diffusion models (Ho et al., 2020). This iterative *sampling operation* implicitly maps a parameter $\theta \in \mathbb{R}^p$ to a distribution $\pi^*(\theta)$.

In this work, our focus is on optimization problems over these implicitly parameterized distributions. For a space of distributions \mathcal{P} (e.g. over \mathbb{R}^d), and a function $\mathcal{F} : \mathcal{P} \rightarrow \mathbb{R}$, our main problem of interest is

$$\min_{\theta \in \mathbb{R}^p} \ell(\theta) := \min_{\theta \in \mathbb{R}^p} \mathcal{F}(\pi^*(\theta))$$

This setting encompasses for instance learning parameter-

*Work mostly done while a student researcher at Google DeepMind [†]Work done while a research scientist at Google DeepMind ¹Institute of Mathematics, EPFL, Lausanne, Switzerland ²ENSAE, CREST, IP Paris, France ³Google DeepMind. Correspondence to: Pierre Marion <pierre.marion@epfl.ch>, Quentin Berthet <qberthet@google.com>.

Preprint under review.

ized Langevin diffusions, contrastive learning of energy-based models (Gutmann & Hyvärinen, 2012) or finetuning denoising diffusion models (e.g., Dvijotham et al., 2023; Clark et al., 2024), as illustrated by Figure 1.

Applying first-order optimizers to this problem raises the challenge of computing gradients of functions of the target distribution with respect to the parameter: we have to *differentiate through a sampling operation*, where the link between θ and $\pi^*(\theta)$ can be *implicit* (see, e.g., Figure 2).

To this aim, we propose to exploit the perspective of *sampling as optimization*, where the task of sampling is seen as an optimization problem over the space of probability distributions \mathcal{P} (see Korba & Salim, 2022, and references therein). Typically, approximating a target probability distribution π can be cast as the minimization of a dissimilarity functional between probability distributions w.r.t. π , that only vanishes at the target. For instance, it is known that Langevin diffusion dynamics follow a gradient flow of a Kullback-Leibler (KL) objective with respect to the Wasserstein-2 distance

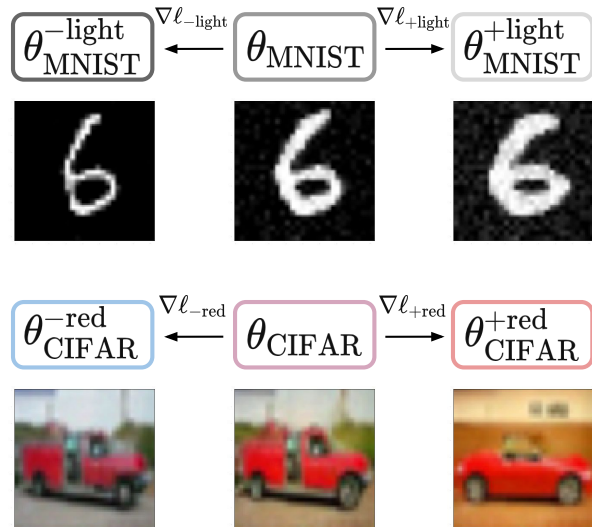


Figure 1. Optimizing through sampling with **Implicit Diffusion** to finetune denoising diffusion models. The reward is the average brightness for MNIST and the red channel average for CIFAR-10.

from optimal transport (Jordan et al., 1998). These dynamics can be discretized to lead to tractable sampling algorithms, like Langevin Monte Carlo (Parisi, 1981; Roberts & Tweedie, 1996; Wibisono, 2018; Durmus et al., 2019).

This allows us to draw a link between optimization through stochastic sampling and *bilevel optimization*, which often involves computing derivatives of the solution of a parameterized optimization problem obtained after iterative steps of an algorithm. Bilevel optimization is an active area of research that finds many relevant applications in machine learning, such as hyperparameter optimization (Franceschi et al., 2018) or meta-learning (Liu et al., 2019). In particular, there is a significant effort in the literature for developing tractable and provably efficient algorithms in a large-scale setting (Pedregosa, 2016; Chen et al., 2021b; Arbel & Mairal, 2022; Blondel et al., 2022; Dagr eou et al., 2022)—see Appendix D for additional related work. This literature focuses mostly on problems where all the variables are finite-dimensional, in contrast with our work where the solution of the inner problem is a distribution in \mathcal{P} .

These motivating similarities, while useful, are not limiting, and we also consider settings where the sampling iterations are not readily interpretable as an optimization algorithm. This more general formulation encompasses for instance diffusion models (Song et al., 2021), that cannot directly be formalized as descent dynamics of an objective functional over \mathcal{P} , but whose output is determined by a parameter θ (i.e. the weights of the neural networks for score matching).

Main Contributions. In this work, we introduce the algorithm of **Implicit Diffusion**, an effective and principled technique for optimizing through a sampling operation. It allows us to train or finetune models that are used to generate samples. Our main contributions are the following:

- We present a general framework describing parameterized sampling algorithms, and introduce Implicit Diffusion optimization, a **single-loop** optimization algorithm to optimize through sampling.
- We analyze the performance of this algorithm, and provide **theoretical guarantees** under various conditions, in the continuous and discrete time settings.
- We showcase its performance in experimental settings.

Notations. For a set \mathcal{X} (such as \mathbb{R}^d), we write \mathcal{P} for the set of probability distributions on \mathcal{X} , omitting reference to \mathcal{X} . For f a differentiable function on \mathbb{R}^d , we denote by ∇f its gradient function, without further indication on the variable unless ambiguous. If f is a differentiable function of k variables, we let $\nabla_i f$ its gradient w.r.t. its i -th variable.

2. Problem presentation

2.1. Sampling and optimization perspectives

The core operation that we consider is sampling by running a stochastic diffusion process that depends on a parameter $\theta \in \mathbb{R}^p$. We consider *iterative sampling operators*, that are mappings from a *parameter space* to a *space of probabilities*. We denote by $\pi^*(\theta) \in \mathcal{P}$ the outcome distribution of this sampling operator. This parameterized distribution is defined in an *implicit* manner since there is not always an explicit way to write down its dependency on θ . More formally, iterative sampling operators are defined as follows.

Definition 2.1 (Iterative sampling operators). For a parameter $\theta \in \mathbb{R}^p$, a sequence of parameterized functions $\Sigma_s(\cdot, \theta)$ from \mathcal{P} to \mathcal{P} defines a diffusion *sampling process*, that starts from $p_0 \in \mathcal{P}$ and iterates

$$p_{s+1} = \Sigma_s(p_s, \theta). \quad (1)$$

The outcome of this process $\pi^*(\theta) \in \mathcal{P}$ (either in the limit when $s \rightarrow \infty$, or for some fixed $s = T$) defines a *sampling operator* $\pi^* : \mathbb{R}^p \rightarrow \mathcal{P}$. \square

We embrace the formalism of stochastic processes as acting on probability distributions. This perspective focuses on the *dynamics* of the distribution $(p_s)_{s \geq 0}$, and allows us to more clearly present our optimization problem and algorithms. In practice, however, in all the examples that we consider, this is realized by an iterative process on some random variable X_s such that $X_s \sim p_s$.

Example 2.2. Consider the process defined by

$$X_{s+1} = X_s - 2\delta(X_s - \theta) + \sqrt{2\delta}B_s,$$

where $X_0 \sim p_0 := \mathcal{N}(\mu_0, \sigma_0^2)$, the B_s are i.i.d. standard Gaussian, and $\delta \in (0, 1)$. This is the discrete-time version of Langevin dynamics for $V(x, \theta) = 0.5(x - \theta)^2$ (see Section 2.2). The dynamics induced on probabilities $p_s = \mathcal{N}(\mu_s, \sigma_s^2)$ are

$$\mu_s = \theta + (1 - 2\delta)^s(\mu_0 - \theta), \quad \sigma_s^2 = 1 + (1 - 2\delta)^{2s}(\sigma_0^2 - 1).$$

The sampling operator for $s \rightarrow \infty$ is therefore defined by $\pi^* : \theta \rightarrow \mathcal{N}(\theta, 1)$. \square

More generally, we may consider the iterates X_s of the process defined for some noise variables $(B_s)_{s \geq 0}$ by

$$X_{s+1} = f_s(X_s, \theta) + B_s. \quad (2)$$

Applying $f_s(\cdot, \theta)$ to $X_s \sim p_s$ implicitly defines a dynamic $\Sigma_s(\cdot, \theta)$ on the distribution. In other words, the dynamics on the variables in (2) induce dynamics on the distributions described in (1). Note that, in the special case of normalizing flows (Kobyzev et al., 2019; Papamakarios et al., 2021), explicit formulas for p_s can be derived and evaluated.

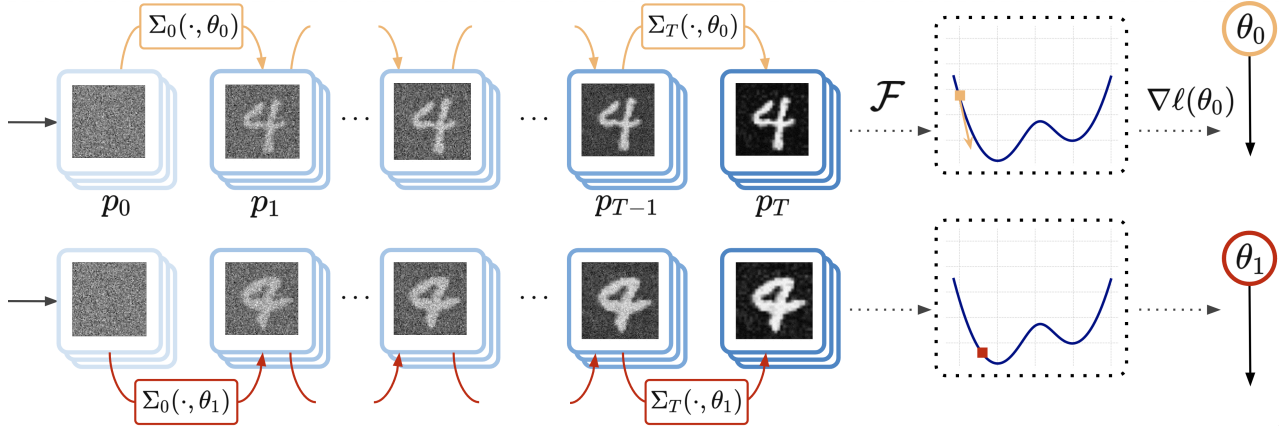


Figure 2. Illustration of one step of optimization through sampling. For a given parameter θ_0 , the sampling process is defined by applying Σ_s for $s \in [T]$, producing $\pi^*(\theta_0)$. The goal of optimization through sampling is to update θ to minimize $\ell = \mathcal{F} \circ \pi^*$. Here the objective \mathcal{F} corresponds to having lighter images (on average), which produces thicker digits.

Remark 2.3. *i)* We consider settings with discrete time steps, since it fits our focus on algorithms to sample and optimize through sampling. This encompasses in particular the discretization of many continuous-time stochastic processes of interest. Most of our motivations are of this type, and we describe these distinctions in our examples (see Section 2.2).

ii) As noted above, these dynamics are often realized by an iterative process on variables X_s , or even on an i.i.d. batch of samples (X_s^1, \dots, X_s^n) . When the iterates $\Sigma_s(p_s, \theta)$ are written in our presentation (e.g. in optimization algorithms in Section 3), it is often a shorthand to mean that we have access to samples from p_s , or equivalently to an empirical version $\hat{p}_s^{(n)}$ of the population distribution p_s . Sample versions of our algorithms are described in Appendix A.

iii) One of the **special cases** considered in our analysis are stationary processes with infinite time horizon, where the sampling operation can be interpreted as optimizing over the set of distributions for some $\mathcal{G} : \mathcal{P} \times \mathbb{R}^p \rightarrow \mathbb{R}$

$$\pi^*(\theta) = \operatorname{argmin}_{p \in \mathcal{P}} \mathcal{G}(p, \theta). \quad (3)$$

In this case, the iterative operations in (1) can often be directly interpreted as descent steps for the objective $\mathcal{G}(\cdot, \theta)$. However, our methodology is **not limited** to this setting: we also consider general sampling schemes with no stationarity and no inner \mathcal{G} , but only a sampling process defined by Σ_s .

Optimization objective. We aim to optimize with respect to θ the output of the sampling operator, for a function $\mathcal{F} : \mathcal{P} \rightarrow \mathbb{R}$. In other words, we consider the optimization problem

$$\min_{\theta \in \mathbb{R}^p} \ell(\theta) := \min_{p \in \mathcal{P}} \mathcal{F}(\pi^*(\theta)). \quad (4)$$

This formulation allows us to transform a problem over distributions in \mathcal{P} to a finite-dimensional problem over $\theta \in$

\mathbb{R}^p . Optimizing a loss over θ allows for convenient post-optimization sampling: for some $\theta_{\text{opt}} \in \mathbb{R}^d$ obtained by solving problem (4) one can sample from $\pi^*(\theta_{\text{opt}})$. This is the common paradigm in model finetuning.

We consider in this work two main examples, quite different in nature, to illustrate and motivate our setting, that we expose next.

2.2. Examples

Langevin dynamics. Langevin dynamics (Roberts & Tweedie, 1996) are defined by the stochastic differential equation (SDE)

$$dX_t = -\nabla_1 V(X_t, \theta) dt + \sqrt{2} dB_t, \quad (5)$$

where V and $\theta \in \mathbb{R}^p$ are such that this SDE has a solution for $t > 0$ that converges in distribution. We consider in this case $\Sigma : \theta \mapsto \pi^*(\theta)$ the limiting distribution of X_t when $t \rightarrow \infty$, given by the Gibbs distributions

$$\pi^*(\theta)[x] = \exp(-V(x, \theta)) / Z_\theta. \quad (6)$$

To fit our setting of iterative sampling algorithms (2), one can consider instead the discretization for small $\gamma > 0$

$$X_{k+1} = X_k - \gamma \nabla_1 V(X_k, \theta) + \sqrt{2\gamma} B_{k+1}.$$

Defining $\mathcal{G}(p, \theta) = \text{KL}(p || \pi^*(\theta))$, we have that both the outcome of the sampling operator $\pi^*(\theta)$ is a minimum of $\mathcal{G}(\cdot, \theta)$, and the SDE (5) implements a gradient flow for \mathcal{G} in the space of measures, with respect to the Wasserstein-2 distance (Jordan et al., 1998). Two optimization objectives \mathcal{F} are of particular interest in this case. First, we may want to maximize some reward $R : \mathbb{R}^d \rightarrow \mathbb{R}$ over our samples, in which case the objective writes $\mathcal{F}(p) := -\mathbb{E}_{x \sim p}[R(x)]$. Second, to approximate a reference distribution p_{ref} with sample access, it is possible to take $\mathcal{F}(p) := \text{KL}(p_{\text{ref}} || p)$.

This case corresponds to training energy-based models (Gutmann & Hyvärinen, 2012). It is also naturally possible to consider a linear combination of these two objectives.

Denoising diffusion. Denoising diffusion (Hyvärinen, 2005; Vincent, 2011; Ho et al., 2020) consists in running the SDE, for $Y_0 \sim \mathcal{N}(0, I)$,

$$dY_t = \{Y_t + 2s_\theta(Y_t, T - t)\}dt + \sqrt{2}dB_t, \quad (7)$$

where $s_\theta : \mathbb{R}^d \times [0, T] \rightarrow \mathbb{R}^d$ is a parameterized *score function*. Its aim is to reverse a forward Ornstein–Uhlenbeck process $dX_t = -X_t dt + \sqrt{2}dB_t$, where we have sample access to $X_0 \sim p_{\text{data}} \in \mathcal{P}$. More precisely, denoting by p_t the distribution of X_t , if $s_\theta \approx \nabla \log p_t$, then the distribution of Y_T is close to p_{data} for large T (Anderson, 1982), which allows approximate sampling from p_{data} .

We are interested in optimizing through diffusion sampling and consider $\pi^*(\theta)$ as the distribution of Y_T . A key example is when θ_0 represents the weights of a model s_{θ_0} that has been pretrained by score matching (aiming to have $\pi^*(\theta_0) \approx p_{\text{data}}$), and one wants to finetune the target distribution $\pi^*(\theta)$, for example in order to increase a reward $R : \mathbb{R}^d \rightarrow \mathbb{R}$. Note that this finetuning step does not require access to p_{data} . As for Langevin dynamics, we consider in our algorithms approximations in discrete time. However in this case, there exists no natural functional \mathcal{G} minimized by the sampling process. An alternative to (7) is the ordinary differential equation (ODE)

$$Y_0 \sim \mathcal{N}(0, I), \quad dY_t = \{Y_t + s_\theta(Y_t, T - t)\}dt. \quad (8)$$

If s_θ is exactly equal to $\nabla \log p_t$, then the solution to both (7) and (8) have the same marginal distributions.

3. Methods

Solving the optimization problem (4) with first-order methods presents several challenges, that we review here. We then introduce an overview of our approach, before getting in the details of our proposed algorithms.

3.1. Overview

Estimation of gradients through sampling. Even given samples from $\pi^*(\theta)$, applying a first-order method to (4) requires computing and evaluating gradients of $\ell := \mathcal{F} \circ \pi^*$. Since there is no closed form for ℓ and no explicit computational graph, the gradient must be evaluated in another fashion, and we consider the following setting.

Definition 3.1 (Implicit gradient estimation). We consider settings where Σ_s, \mathcal{F} are such that the gradient of ℓ can be *implicitly estimated*: there is a function $\Gamma : \mathcal{P} \times \mathbb{R}^p \rightarrow \mathbb{R}^p$ such that $\nabla \ell(\theta) = \Gamma(\pi^*(\theta), \theta)$. \square

Indeed, in practice we rarely reach exactly the distribution $\pi^*(\theta)$, e.g. because a finite number of iterations of sampling is performed. Then, if $\hat{\pi} \approx \pi^*(\theta)$, the gradient can be approximated by $\hat{g} = \Gamma(\hat{\pi}, \theta)$. Hence, given access to approximate samples of $\pi^*(\theta)$, it is possible to compute an estimate of $\nabla \ell(\theta)$, and this is at the heart of our methods—see Appendix A.1 for more detailed discussion. There are several settings where such a Γ exists, and examples are given in Section 3.2. Note that when Γ is linear in its first argument, sample access to $\pi^*(\theta)$ yields unbiased estimates of the gradient. This case has been studied with various approaches (see Sutton et al., 1999; Fu & Hu, 2012; Pflug, 2012; De Bortoli et al., 2021 and Appendix D).

Beyond nested-loop approaches. Sampling from $\pi^*(\theta)$ is usually only feasible via iterations of the sampling process Σ_s . The most straightforward method is then a nested loop: at each optimization step k , running an inner loop for a large amount T of steps of Σ_s as in (1) to produce $\hat{\pi}_k \approx \pi^*(\theta_k)$, and using it to evaluate a gradient. We formalize this method for comparison purposes in Algorithm 1.

Algorithm 1 Vanilla nested-loop approach (Baseline)

```

input  $\theta_0 \in \mathbb{R}^p, p_0 \in \mathcal{P}$ 
for  $k \in \{0, \dots, K - 1\}$  (outer optimization loop) do
   $p_k^{(0)} \leftarrow p_0$ 
  for  $s \in \{0, \dots, T - 1\}$  (inner sampling loop) do
     $p_k^{(s+1)} \leftarrow \Sigma_s(p_k^{(s)}, \theta_k)$ 
   $\hat{\pi}_k \leftarrow p_k^{(T)}$ 
   $\theta_{k+1} \leftarrow \theta_k - \eta \Gamma(\hat{\pi}_k, \theta_k)$  (or another optimizer)
output  $\theta_K$ 

```

This approach can be inefficient for two reasons: first, it requires solving the inner sampling problem *at each optimization step*. Further, nested loops are typically impractical with modern accelerator-oriented computing hardware. These challenges can be partially alleviated by techniques like gradient checkpointing (see Appendix D for references).

We rather step away from the nested-loop paradigm and follow a different approach inspired by methods in bilevel optimization, aiming to *jointly* iterate on both the sampling problem (evaluation of π^* —the inner problem), and the optimization problem over $\theta \in \mathbb{R}^p$ (the outer objective \mathcal{F}). We describe these methods in Section 3.3 and Algorithms 2 and 3. The connection with bilevel optimization is especially seamless when sampling can indeed be cast as an optimization problem over distributions in \mathcal{P} , as in (3). However, as noted above, our approach generalizes beyond this case.

3.2. Methods for gradient estimation through sampling

We explain how to perform implicit gradient estimation as in Definition 3.1, that is, how to derive expressions for the

function Γ , in several cases of interest.

Direct analytical derivation. In the case of Langevin dynamics, it is possible to derive analytical expressions for Γ depending on the outer objective \mathcal{F} . We illustrate this idea for the two objectives introduced in Section 2.2. First, in the case where $\mathcal{F}(p) = -\mathbb{E}_{x \sim p}[R(x)]$, a straightforward derivation detailed in Appendix A.2 shows that

$$\nabla \ell_{\text{reward}}(\theta) = \text{Cov}_{X \sim \pi^*(\theta)}[R(X), \nabla_2 V(X, \theta)].$$

Recalling Definition 3.1, this suggests taking Γ as

$$\Gamma_{\text{reward}}(p, \theta) := \text{Cov}_{X \sim p}[R(X), \nabla_2 V(X, \theta)]. \quad (9)$$

Note that this formula does not involve gradients of R , hence our approach handles non-differentiable rewards.

Second, consider the case where $\mathcal{F}(p) = \text{KL}(p_{\text{ref}} || p)$. We then have, following Gutmann & Hyvärinen (2012),

$$\nabla \ell_{\text{ref}}(\theta) = \mathbb{E}_{X \sim p_{\text{ref}}}[\nabla_2 V(X, \theta)] - \mathbb{E}_{X \sim \pi^*(\theta)}[\nabla_2 V(X, \theta)].$$

This is known as contrastive learning when p_{ref} is given by data, and suggests taking Γ as

$$\Gamma_{\text{ref}}(p, \theta) := \mathbb{E}_{X \sim p_{\text{ref}}}[\nabla_2 V(X, \theta)] - \mathbb{E}_{X \sim p}[\nabla_2 V(X, \theta)]. \quad (10)$$

This extends naturally to linear combinations of Γ_{reward} and Γ_{ref} .

Implicit differentiation. When $\pi^*(\theta) = \text{argmin} \mathcal{G}(\cdot, \theta)$ as in (3), under generic assumptions on \mathcal{G} , the implicit function theorem (see Krantz & Parks, 2002; Blondel et al., 2022 and Appendix A.4) shows that $\nabla \ell(\theta) = \Gamma(\pi^*(\theta), \theta)$ with

$$\Gamma(p, \theta) = \int \mathcal{F}'(p)[x] \gamma(p, \theta)[x] dx.$$

Here $\mathcal{F}'(p) : \mathcal{X} \rightarrow \mathbb{R}$ denotes the first variation of \mathcal{F} at $p \in \mathcal{P}$ (see Definition B.1) and $\gamma(p, \theta)$ is the solution of the linear system

$$\int \nabla_{1,1} \mathcal{G}(p, \theta)[x, x'] \gamma(p, \theta)[x'] dx' = -\nabla_{1,2} \mathcal{G}(p, \theta)[x].$$

Although this gives us a general way to define gradients of $\pi^*(\theta)$ with respect to θ , solving this linear system is generally not feasible. One exception is when sampling over a finite state space \mathcal{X} , in which case \mathcal{P} is finite-dimensional, and the integrals boil down to matrix-vector products.

Differential adjoint method. The adjoint method allows computing gradients through differential equation solvers (Pontryagin, 1987; Li et al., 2020), applying in particular for denoising diffusion. It can be connected to implicit differentiation, by defining \mathcal{G} over a measure path instead of a single measure p (see, e.g., Kidger, 2022).

To introduce the adjoint method, consider the ODE $dY_t = \mu(t, Y_t, \theta) dt$ integrated between 0 and some $T > 0$. This setting encompasses the denoising diffusion ODE (8) with the appropriate choice of μ . Assume that the outer objective \mathcal{F} writes as the expectation of some differentiable reward R , namely $\mathcal{F}(p) = \mathbb{E}_{x \sim p}[R(x)]$. Considering the ODE system

$$\begin{aligned} Z_0 &\sim p, & dZ_t &= -\mu(t, Z_t, \theta) dt, \\ A_0 &= \nabla R(Z_0), & dA_t &= A_t^\top \nabla_2 \mu(T - t, Z_t, \theta) dt, \\ G_0 &= 0, & dG_t &= A_t^\top \nabla_3 \mu(T - t, Z_t, \theta) dt, \end{aligned}$$

and defining $\Gamma(p, \theta) := G_T$, the adjoint method shows that $\Gamma(\pi^*(\theta), \theta)$ is an unbiased estimate of $\nabla \ell(\theta)$. We refer to Appendix A.3 for details and explanations on how to differentiate through the SDE sampler (7) and to incorporate a KL term in the reward by using Girsanov's theorem.

3.3. Implicit Diffusion optimization algorithm

Our **proposed approach** is to circumvent solving the inner problem in Algorithm 1 (i.e. sample exactly or approximately from $\pi^*(\theta_k)$ at each update of θ_k). We propose a **joint single-loop approach** that keeps track of a single dynamic of probabilities $(p_k)_{k \geq 0}$. At each optimization step, the probability p_k is updated with one sampling step depending on the current parameter θ_k , as detailed in Algorithm 2. As noted in Section 3.1, there are parallels with some approaches in the literature in the linear case, but our method goes beyond in making no linearity assumption on Γ .

Algorithm 2 Implicit Diff. optimization, infinite time

input $\theta_0 \in \mathbb{R}^p, p_0 \in \mathcal{P}$
for $k \in \{0, \dots, K - 1\}$ (joint single loop) **do**
 $p_{k+1} \leftarrow \Sigma_k(p_k, \theta_k)$
 $\theta_{k+1} \leftarrow \theta_k - \eta \Gamma(p_k, \theta_k)$ (or another optimizer)
output θ_K

This point of view is well-suited for stationary processes with infinite-time horizon, but does not apply directly to sampling with diffusions with a finite-time horizon (and no stationary property), which cannot be run for an arbitrary number of steps. We show next how to adapt our approach.

Finite time-horizon: queuing trick. When $\pi^*(\theta)$ is obtained or approximated by a large, but *finite* number T of iterations of the operator Σ_s , we propose to leverage hardware parallelism to evaluate in parallel several, say M , dynamics of the distribution p_k , through a queue of length M . We present for simplicity in Figure 3 and in Algorithm 3 the case where $M = T$ and discuss extensions in Appendix A.3. At each step, the M -th element of the queue $p_k^{(M)}$ provides a distribution to update θ through evaluation of Γ .

Updating a single dynamic of probabilities $(p_k)_{k \geq 0}$ would only provide a single gradient estimate (after T sampling

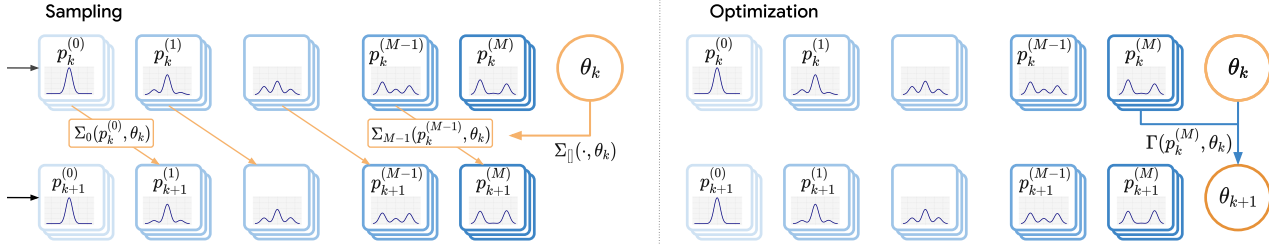


Figure 3. Illustration of the Implicit Diffusion optimization algorithm, in the finite time setting. Left: Sampling - one step of the parameterized sampling scheme is applied in parallel to all distributions in the queue. Right: Optimization - the last element of the queue is used to compute a gradient for the parameter.

steps), which is why Algorithm 2 would not work in this case. Moreover, leveraging parallelism, the running time of our algorithm is $\mathcal{O}(K)$, gaining a factor of T compared to the nested-loop approach. We show in Section 4 and 5 its performance in theoretical and experimental settings.

Algorithm 3 Implicit Diff. optimization, finite time

input $\theta_0 \in \mathbb{R}^p, p_0 \in \mathcal{P}$
input $P_M = [p_0^{(0)}, \dots, p_0^{(M)}]$
for $k \in \{0, \dots, K-1\}$ (joint single loop) **do**
 $p_{k+1}^{(0)} \leftarrow p_0$
parallel $p_{k+1}^{(m+1)} \leftarrow \Sigma_m(p_k^{(m)}, \theta_k)$ for $m \in [M-1]$
 $\theta_{k+1} \leftarrow \theta_k - \eta \Gamma(p_k^{(M)}, \theta_k)$ (or another optimizer)
output θ_K

4. Theoretical analysis

We analyze continuous and discrete Langevin sampling and a case of denoising diffusion. Proofs are in Appendix B.

4.1. Langevin with continuous flow

The continuous-time equivalent of Algorithm 2 in the case of Langevin dynamics writes

$$dX_t = -\nabla_1 V(X_t, \theta_t) dt + \sqrt{2} dB_t, \quad (11)$$

$$d\theta_t = -\varepsilon_t \Gamma(p_t, \theta_t) dt, \quad (12)$$

where p_t denotes the distribution of X_t . We recall that in practice $\Gamma(p_t, \theta_t)$ is approximated on a finite sample, making the dynamics (12) stochastic. We leave the theoretical analysis of stochastic dynamics on θ_t for future work. Note that $\varepsilon_t > 0$ corresponds to the ratio of learning rates between the inner and the outer problems. Our analysis uses that the outer variable evolves slowly with respect to the inner variable, which is the case when ε_t is small enough. This reasoning, sometimes referred to as *two-timescale analysis* of gradient flow, was already used to tackle non-convex optimization problems in machine learning (Heusel et al., 2017; Arbel & Mairal, 2022; Dagr eou

et al., 2022; Hong et al., 2023; Marion & Berthier, 2023). Recalling that $\pi^*(\theta) = \exp(-V(\cdot, \theta))/Z_\theta$ is the stationary distribution of (11), we require the following assumption.

Assumption 4.1. $\pi^*(\theta_t)$ verifies the Log-Sobolev inequality with constant $\mu > 0$ for all $t \geq 0$, i.e., for all $p \in \mathcal{P}$,

$$\text{KL}(p \parallel \pi^*(\theta_t)) \leq \frac{1}{2\mu} \left\| \nabla \log \left(\frac{p}{\pi^*(\theta)} \right) \right\|_{L^2(p)}^2.$$

Remark that μ -strong convexity of the potentials $(V(\cdot, \theta_t))_{t \geq 0}$ implies Assumption 4.1, but the latter is more general (Vempala & Wibisono, 2019), including for instance distributions π whose potential are bounded perturbations of a strongly convex potential (Bakry et al., 2014).

We also assume that the gradients of the potential V w.r.t. the outer variable are uniformly bounded, namely

Assumption 4.2. The potential V is continuously differentiable and for $\theta \in \mathbb{R}^p, x \in \mathbb{R}^d, \|\nabla_2 V(x, \theta)\| \leq C$.

Assumptions 4.1 and 4.2 hold for example when the potential defines a mixture of Gaussians and the parameters θ determine the weights of the mixture. We refer to Appendix B.1.2 for a precise statement and proof.

We also assume that the outer problem updates are bounded and Lipschitz continuous, in the sense of the KL divergence.

Assumption 4.3. For all $p \in \mathcal{P}, q \in \mathcal{P}, \theta \in \mathbb{R}^p$,

$$\|\Gamma(p, \theta)\| \leq C \text{ and } \|\Gamma(p, \theta) - \Gamma(q, \theta)\| \leq K_\Gamma \sqrt{\text{KL}(p \parallel q)}.$$

The next proposition shows that this assumption holds for the examples of interest given in Section 2.

Proposition 4.4. Consider a bounded function $R: \mathbb{R}^d \rightarrow \mathbb{R}$. Then, under Assumption 4.2, the functions Γ_{reward} and Γ_{ref} defined by (9)–(10) satisfy Assumption 4.3.

Since we make no assumption of strong convexity on Γ or ℓ , we cannot hope to prove convergence of the gradient flow to a global minimizer of the objective. Instead, we show convergence of the average of the objective gradients.

Theorem 4.5. Take $\varepsilon_t = \min(1, \frac{1}{\sqrt{t}})$. Then, under Assumptions 4.1, 4.2, and 4.3,

$$\frac{1}{T} \int_0^T \|\nabla \ell(\theta_t)\|^2 dt \leq \frac{c(\ln T)^2}{T^{1/2}}$$

for some $c > 0$ depending on the constants of the problem.

The proof starts by noticing that the updates (12) in θ would follow the gradient flow for ℓ if $p_t = \pi^*(\theta_t)$. Since the sampling problem is not solved perfectly, the equality does not hold. We can still bound the deviation with the gradient flow dynamics by an error term involving the KL divergence of p_t from $\pi^*(\theta_t)$. Next, this KL can be bounded since the updates (11) in X_t are gradient steps for the KL (see Section 2.2). However, while p_t moves towards $\pi^*(\theta_t)$ with the updates (11) in X_t , $\pi^*(\theta_t)$ may be moving away due to the updates (12) in θ_t . We can still obtain convergence of p_t to $\pi^*(\theta_t)$ by requiring the ratio of learning rates ε_t to decay.

4.2. Langevin with discrete flow

We now consider the discrete version of (11)–(12), namely

$$X_{k+1} = X_k - \gamma_k \nabla_1 V(X_k, \theta_k) + \sqrt{2\gamma_k} B_{k+1}, \quad (13)$$

$$\theta_{k+1} = \theta_k - \gamma_k \varepsilon_k \Gamma(p_k, \theta_k), \quad (14)$$

where p_k denotes the distribution of X_k . This setting is more challenging because of the bias introduced by discretizing the Langevin diffusion (Wibisono, 2018). We next make smoothness assumptions that are classical to analyze (discrete) gradient descent (e.g., Vempala & Wibisono, 2019).

Assumption 4.6. The functions $\nabla_1 V(\cdot, \theta)$, $\nabla_1 V(x, \cdot)$ and $\nabla \ell$ are respectively L_X -Lipschitz for all $\theta \in \mathbb{R}^p$, L_Θ -Lipschitz for all $x \in \mathbb{R}^d$, and L -Lipschitz.

We can then show the following convergence result.

Theorem 4.7. Take $\gamma_k = \frac{c_1}{\sqrt{k}}$ and $\varepsilon_k = \frac{1}{\sqrt{k}}$. Then, under Assumptions 4.1, 4.2, 4.3, and 4.6,

$$\frac{1}{K} \sum_{k=1}^K \|\nabla \ell(\theta_k)\|^2 \leq \frac{c_2 \ln K}{K^{1/3}},$$

where $c_1, c_2 > 0$ depend on the constants of the problem.

The proof follows a similar outline as in the continuous case. However, in bounding the KL divergence of p_k from $\pi^*(\theta_k)$, we incur an additional discretization error term proportional to γ_k . This term, which we bound by making γ_k decay to zero, induces a slower convergence rate. The proof technique to bound the KL in discrete iterations is inspired by Vempala & Wibisono (2019). We obtain a result similar to Dagr eou et al. (2022, Theorem 2) for finite-dimensional bilevel optimization, albeit with a slower convergence rate.

4.3. Denoising diffusion

The analysis of denoising diffusion and of Algorithm 3 is more challenging since the distribution $\pi^*(\theta)$ can not be readily characterized as the stationary point of an iterative process, hence the previous proof technique does not adapt. We study a one-dimensional Gaussian case and leave more general analysis for future work. Considering $p_{\text{data}} = \mathcal{N}(\theta_{\text{data}}, 1)$ and the forward process of Section 2.2, the score is $\nabla \log p_t(x) = -(x - \theta_{\text{data}} e^{-t})$. A natural score function is therefore $s_\theta(x, t) := -(x - \theta e^{-t})$. With this score function, the output of the sampling process (7) is

$$\pi^*(\theta) = \mathcal{N}(\theta(1 - e^{-2T}), 1).$$

Remarkably, $\pi^*(\theta)$ is a Gaussian distribution for all $\theta \in \mathbb{R}$, making the analytical study of this model tractable.

Assume that pretraining with samples of p_{data} outputs a value $\theta = \theta_0$ (supposedly close to θ_{data}), and we want to finetune the model towards some other $\theta_{\text{target}} \in \mathbb{R}$ by optimizing the reward $R(x) = -(x - \theta_{\text{target}})^2$. A short computation shows that, in this case, $\nabla \ell(\theta) = -\mathbb{E}_{x \sim \pi^*(\theta)} R'(x)(1 - e^{-2T})$, hence one can take $\Gamma(p, \theta) = -\mathbb{E}_{x \sim p} R'(x)(1 - e^{-2T})$. It is then possible to study a continuous-time equivalent of Algorithm 3, where Σ corresponds to the denoising diffusion sampling (7) and Γ is given above. One can then show

Proposition 4.8. (informal) Let $(\theta_t)_{t \geq 0}$ be given by the continuous-time equivalent of Algorithm 3. Then

$$\|\theta_{2T} - \theta_{\text{target}}\| = \mathcal{O}(e^{-T}),$$

and $\pi^*(\theta_{2T}) = \mathcal{N}(\mu_{2T}, 1)$ with $\mu_{2T} = \theta_{\text{target}} + \mathcal{O}(e^{-T})$.

This shows that Algorithm 3 is able to bias the parameter towards θ_{target} . We refer to Appendix B.3 for more detailed explanations, statement of the Proposition and proof.

5. Experiments

We illustrate the performance of the Implicit Diffusion algorithm. Experimental details are given in Appendix C.

5.1. Reward training of Langevin processes

We consider the case of Langevin processes (see Section 2.2) where the potential $V(\cdot, \theta)$ is a logsumexp of quadratics—so that the outcome distributions are mixtures of Gaussians. We optimize the reward $R(x) = \mathbf{1}(x_1 > 0) \exp(-\|x - \mu\|^2)$, for $\mu \in \mathbb{R}^d$, thereby illustrating the ability of our method to optimize even reward functions that are not differentiable.

We run four sampling algorithms, including the infinite time-horizon version of **Implicit Diffusion** (Algorithm 2), all starting from $p_0 = \mathcal{N}(0, I_d)$ and for $T = 5,000$ steps.

- Langevin θ_0 (■): Langevin diffusion (5) with potential $V(\cdot, \theta_0)$ for some fixed $\theta_0 \in \mathbb{R}^p$, no reward.

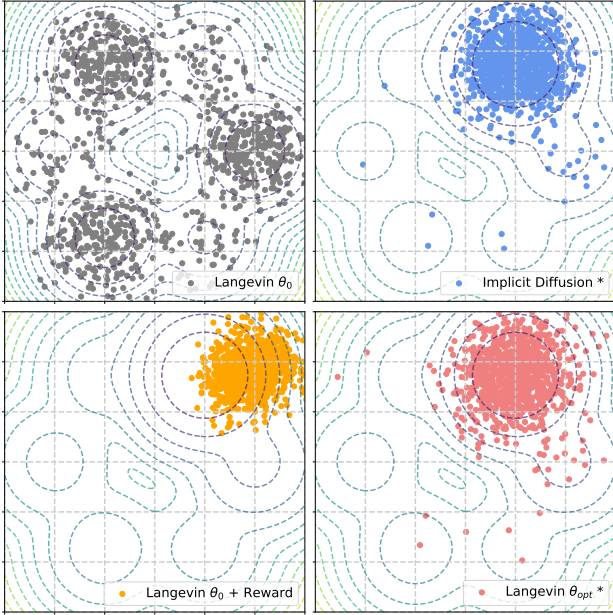


Figure 4. Contour lines and samples from sampling algorithms (see details in Section 5.1). **Top left:** Langevin θ_0 (●) with $\pi^*(\theta_0)$ contour lines **Top right:** Implicit Diffusion (●) with $\pi^*(\theta_{\text{opt}})$ contour lines. **Bottom left:** Langevin θ_0 + smoothed Reward (●). **Bottom right:** Langevin θ_{opt} (●).

- Implicit Diffusion (★): with $\mathcal{F}(p) = -\mathbb{E}_{X \sim p}[R(X)]$, yielding both a sample \hat{p}_T and parameters θ_{opt} .
- Langevin $\theta_0 + R$ (▼): (5) with $V(\cdot, \theta_0) - \lambda R_{\text{smooth}}$ potential, where R_{smooth} is a smoothed version of R .
- Langevin θ_{opt} (●): (5) with potential $V(\cdot, \theta_{\text{opt}})$. This is inference post-training with Implicit Diffusion.

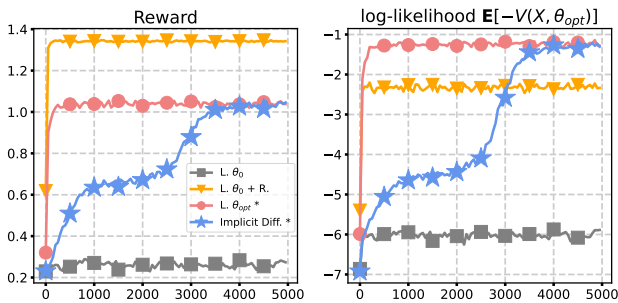


Figure 5. Metrics for reward training of Langevin processes (see Section 5.1), both averaged on a batch. **Left:** The average reward on the sample distribution, at each step. **Right:** The average log-likelihood of $\pi^*(\theta_{\text{opt}})$ on the sample distribution, at each step.

Both qualitatively (Figure 4) and quantitatively (Figure 5), we observe that our approach allows us to efficiently optimize through sampling, and learn a parameter: after T steps, our algorithm yields both $\theta_{\text{opt}} := \theta_T$ and a sample \hat{p}_T approximately from $\pi^*(\theta_{\text{opt}})$. Then, it is convenient and fast to

sample post hoc, with a Langevin process using θ_{opt} —as observed in Figure 5. This is similar in spirit to inference with a finetuned model, post-reward training. We also observe that directly adding a reward term to a Langevin process is less efficient: it tends to overfit on the reward, as the target distribution of this process is out of the family of $\pi^*(\theta)$'s.

5.2. Reward training of denoising diffusion models

We also apply **Implicit Diffusion** for reward finetuning of denoising diffusion models pretrained on image datasets. We denote by θ_0 the weights of a model pretrained on these datasets, such that $\pi^*(\theta_0) \approx p_{\text{data}}$. For various reward functions on the samples $R : \mathbb{R}^d \rightarrow \mathbb{R}$, we consider

$$\mathcal{F}(p) := -\lambda \mathbb{E}_{x \sim p}[R(x)] + \beta \text{KL}(p || \pi^*(\theta_0)),$$

common in reward finetuning (see, e.g., Ziegler et al., 2019, and references therein). We run **Implicit Diffusion** using the finite time-horizon variant described in Algorithm 3, applying the adjoint method on SDEs for gradient estimation. We report samples generated by $\pi^*(\theta_t)$, as well as reward and KL divergence estimates (see Figures 1 and 6).

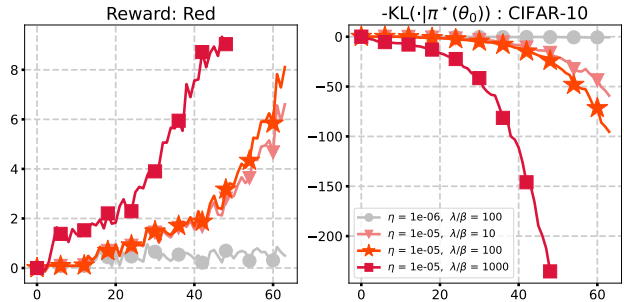


Figure 6. Score function reward training with **Implicit Diffusion** (CIFAR-10 pretrained) for various $\lambda, \eta > 0$. **Left:** Reward, average of the red channel minus the average of the others. **Right:** Divergence w.r.t. the distribution after pretraining.

We report results on two models pretrained on the image datasets MNIST (LeCun & Cortes, 1998) and CIFAR-10 (Krizhevsky, 2009). For pretraining, we follow the method of Hoogeboom et al. (2023) and use U-Net models (Ronneberger et al., 2015). We display visual examples in Figure 1 and in Appendix C, where we also report some metrics. While the finetuned models diverge from the original distribution—since some statistics are shifted by reward training, they retain overall semantic information (e.g. brighter digits are thicker, rather than on a gray background).

MNIST. We pretrain a 2.5M parameters model for 18k steps in 7 minutes on 4 TPUv2, without label conditioning. For reward training, our reward is the average brightness (i.e. average of all pixel values), for positive and negative values of λ . We train on a TPUv2 for 4 hours with a queue of size $M = 4$, $T = 64$ steps, and a batch size of 32.

CIFAR-10. We pretrain a 53.2M parameters model for 500k steps in 30 hours on 16 TPUv2, with label conditioning, reaching an FID score (Heusel et al., 2017) of 2.5. For reward training, our reward is the average brightness of the red channel minus the average on the other channels, for positive and negative values of λ . We train on a TPUv3 for 9 hours with a queue of size $M = 4$ and $T = 64$ steps, and a batch size of 32. We observe in Figure 6 the high impact of the learning rate, and the competition between the reward and the divergence to the distribution after pretraining.

Impact statement

This paper presents work whose goal is to advance the field of Machine Learning. There are many potential societal consequences of our work, none which we feel must be specifically highlighted here.

Author contribution statement

PM worked on designing the methodology, implemented the codebase for experiments, proved theoretical guarantees for proposed method, contributed importantly to writing the paper. AK contributed to designing the methodology, worked on proving theoretical guarantees, made some contributions to the paper. PB, MB, VDB, AD, FL, CP (by alphabetical order) contributed to discussions in designing the methodology, provided references, made remarks and suggestions on the manuscript and provided some help with the codebase implementation. QB proposed the initial idea, proposed the general methodology and worked on designing it, contributed to the codebase implementation, ran experiments, and contributed importantly to writing the paper.

Acknowledgments

The authors would like to thank Fabian Pedregosa for very fruitful discussions on implicit differentiation and bilevel optimization that led to this project, Vincent Roulet for very insightful notes and comments about early drafts of this work as well as help with experiment implementation, and Emiel Hoogeboom for extensive help on pretraining diffusion models. PM and AK thank Google for their academic support in the form respectively of a Google PhD Fellowship and a gift in support of her academic research.

References

Ambrosio, L., Gigli, N., and Savaré, G. *Gradient flows: in metric spaces and in the space of probability measures*. Springer Science & Business Media, 2005.

Anderson, B. D. O. Reverse-time diffusion equation models. *Stochastic Processes and their Applications*, 12(3):313–

326, 1982.

Arbel, M. and Mairal, J. Amortized implicit differentiation for stochastic bilevel optimization. In *International Conference on Learning Representations*, 2022.

Atchadé, Y. F., Fort, G., and Moulines, E. On perturbed proximal gradient algorithms. *The Journal of Machine Learning Research*, 18(1):310–342, 2017.

Bakry, D., Gentil, I., Ledoux, M., et al. *Analysis and geometry of Markov diffusion operators*, volume 103. Springer, 2014.

Black, K., Janner, M., Du, Y., Kostrikov, I., and Levine, S. Training diffusion models with reinforcement learning. In *The Twelfth International Conference on Learning Representations*, 2024.

Blondel, M., Berthet, Q., Cuturi, M., Frostig, R., Hoyer, S., Llinares-López, F., Pedregosa, F., and Vert, J.-P. Efficient and modular implicit differentiation. *Advances in neural information processing systems*, 35:5230–5242, 2022.

Bradbury, J., Frostig, R., Hawkins, P., Johnson, M. J., Leary, C., Maclaurin, D., Necula, G., Paszke, A., VanderPlas, J., Wanderman-Milne, S., and Zhang, Q. JAX: composable transformations of Python+NumPy programs, 2018. URL <http://github.com/google/jax>.

Chen, H.-B., Chewi, S., and Niles-Weed, J. Dimension-free log-sobolev inequalities for mixture distributions. *Journal of Functional Analysis*, 281(11):109236, 2021a.

Chen, T., Sun, Y., and Yin, W. Closing the gap: Tighter analysis of alternating stochastic gradient methods for bilevel problems. In Ranzato, M., Beygelzimer, A., Dauphin, Y., Liang, P. S., and Vaughan, J. W. (eds.), *Advances in Neural Information Processing Systems*, volume 34, pp. 25294–25307. Curran Associates, Inc., 2021b.

Chen, T., Sun, Y., Xiao, Q., and Yin, W. A single-timescale method for stochastic bilevel optimization. In *International Conference on Artificial Intelligence and Statistics*, pp. 2466–2488. PMLR, 2022.

Clark, K., Vicol, P., Swersky, K., and Fleet, D. Directly fine-tuning diffusion models on differentiable rewards. In *The Twelfth International Conference on Learning Representations*, 2024.

Dagréou, M., Ablin, P., Vaiter, S., and Moreau, T. A framework for bilevel optimization that enables stochastic and global variance reduction algorithms. In Koyejo, S., Mohamed, S., Agarwal, A., Belgrave, D., Cho, K., and Oh, A. (eds.), *Advances in Neural Information Processing Systems*, volume 35, pp. 26698–26710. Curran Associates, Inc., 2022.

- De Bortoli, V., Durmus, A., Pereyra, M., and Vidal, A. F. Efficient stochastic optimisation by unadjusted langevin monte carlo: Application to maximum marginal likelihood and empirical bayesian estimation. *Statistics and Computing*, 31:1–18, 2021.
- Dhariwal, P. and Nichol, A. Diffusion models beat GANs on image synthesis. In Ranzato, M., Beygelzimer, A., Dauphin, Y., Liang, P. S., and Vaughan, J. W. (eds.), *Advances in Neural Information Processing Systems*, volume 34, pp. 8780–8794. Curran Associates, Inc., 2021.
- Dong, H., Xiong, W., Goyal, D., Zhang, Y., Chow, W., Pan, R., Diao, S., Zhang, J., SHUM, K., and Zhang, T. RAFT: Reward ranked finetuning for generative foundation model alignment. *Transactions on Machine Learning Research*, 2023. ISSN 2835-8856.
- Durmus, A., Majewski, S., and Miasojedow, B. Analysis of langevin monte carlo via convex optimization. *The Journal of Machine Learning Research*, 20(1):2666–2711, 2019.
- Dvijotham, K. D., Omidshafiei, S., Lee, K., Collins, K. M., Ramachandran, D., Weller, A., Ghavamzadeh, M., Nasr, M., Fan, Y., and Liu, J. Z. Algorithms for optimal adaptation of diffusion models to reward functions. In *ICML Workshop on New Frontiers in Learning, Control, and Dynamical Systems*, 2023.
- Eberle, A. Reflection couplings and contraction rates for diffusions. *Probability theory and related fields*, 166: 851–886, 2016.
- Fan, Y., Watkins, O., Du, Y., Liu, H., Ryu, M., Boutilier, C., Abbeel, P., Ghavamzadeh, M., Lee, K., and Lee, K. Dpok: Reinforcement learning for fine-tuning text-to-image diffusion models. *arXiv preprint arXiv:2305.16381*, 2023.
- Franceschi, L., Frascioni, P., Salzo, S., Grazi, R., and Pontil, M. Bilevel programming for hyperparameter optimization and meta-learning. In Dy, J. and Krause, A. (eds.), *Proceedings of the 35th International Conference on Machine Learning*, volume 80 of *Proceedings of Machine Learning Research*, pp. 1568–1577. PMLR, 10–15 Jul 2018.
- Fu, M. C. and Hu, J.-Q. *Conditional Monte Carlo: Gradient estimation and Optimization Applications*, volume 392. Springer Science & Business Media, 2012.
- Griewank, A. and Walther, A. *Evaluating derivatives: principles and techniques of algorithmic differentiation*. SIAM, 2008.
- Guo, Z., Xu, Y., Yin, W., Jin, R., and Yang, T. A novel convergence analysis for algorithms of the adam family and beyond. *arXiv preprint arXiv:2104.14840*, 2021.
- Gutmann, M. U. and Hyvärinen, A. Noise-contrastive estimation of unnormalized statistical models, with applications to natural image statistics. *Journal of machine learning research*, 13(2), 2012.
- Heusel, M., Ramsauer, H., Unterthiner, T., Nessler, B., and Hochreiter, S. GANs trained by a two time-scale update rule converge to a local nash equilibrium. In Guyon, I., Luxburg, U. V., Bengio, S., Wallach, H., Fergus, R., Vishwanathan, S., and Garnett, R. (eds.), *Advances in Neural Information Processing Systems*, volume 30. Curran Associates, Inc., 2017.
- Ho, J., Jain, A., and Abbeel, P. Denoising diffusion probabilistic models. In *Advances in Neural Information Processing Systems*, volume 33, pp. 6840–6851. Curran Associates, Inc., 2020.
- Hong, M., Wai, H.-T., Wang, Z., and Yang, Z. A two-timescale stochastic algorithm framework for bilevel optimization: Complexity analysis and application to actor-critic. *SIAM Journal on Optimization*, 33(1):147–180, 2023.
- Hoogeboom, E., Heek, J., and Salimans, T. simple diffusion: End-to-end diffusion for high resolution images. In *Proceedings of The 40th International Conference on Machine Learning*, 2023.
- Hyvärinen, A. Estimation of non-normalized statistical models by score matching. *Journal of Machine Learning Research*, 6(24):695–709, 2005.
- Jordan, R., Kinderlehrer, D., and Otto, F. The variational formulation of the fokker–planck equation. *SIAM journal on mathematical analysis*, 29(1):1–17, 1998.
- Kidger, P. On neural differential equations. *arXiv preprint arXiv:2202.02435*, 2022.
- Kidger, P., Foster, J., Li, X. C., and Lyons, T. Efficient and accurate gradients for neural SDEs. In Ranzato, M., Beygelzimer, A., Dauphin, Y., Liang, P. S., and Vaughan, J. W. (eds.), *Advances in Neural Information Processing Systems*, volume 34, pp. 18747–18761. Curran Associates, Inc., 2021.
- Kingma, D. and Ba, J. Adam: A method for stochastic optimization. In *International Conference on Learning Representations*, 2015.
- Kobyzev, I., Prince, S., and Brubaker, M. A. Normalizing flows: Introduction and ideas. *stat*, 1050:25, 2019.
- Korba, A. and Salim, A. Sampling as first-order optimization over a space of probability measures, 2022. Tutorial at ICML 2022. Accessible at <https://akorba.github.io/resources/>

- [Baltimore_July2022_ICMLtutorial.pdf](#), consulted on 01/30/2024.
- Krantz, S. G. and Parks, H. R. *The implicit function theorem: history, theory, and applications*. Springer Science & Business Media, 2002.
- Krizhevsky, A. Learning multiple layers of features from tiny images. Technical report, University of Toronto, 2009.
- Kuntz, J., Lim, J. N., and Johansen, A. M. Particle algorithms for maximum likelihood training of latent variable models. In *International Conference on Artificial Intelligence and Statistics*, pp. 5134–5180. PMLR, 2023.
- LeCun, Y. and Cortes, C. MNIST handwritten digit database, 1998. URL <http://yann.lecun.com/exdb/mnist/>.
- Lee, K., Liu, H., Ryu, M., Watkins, O., Du, Y., Boutilier, C., Abbeel, P., Ghavamzadeh, M., and Gu, S. S. Aligning text-to-image models using human feedback. *arXiv preprint arXiv:2302.12192*, 2023.
- Li, X., Wong, T.-K. L., Chen, R. T. Q., and Duvenaud, D. K. Scalable gradients and variational inference for stochastic differential equations. In Zhang, C., Ruiz, F., Bui, T., Dieng, A. B., and Liang, D. (eds.), *Proceedings of The 2nd Symposium on Advances in Approximate Bayesian Inference*, volume 118 of *Proceedings of Machine Learning Research*, pp. 1–28. PMLR, 08 Dec 2020.
- Liu, H., Simonyan, K., and Yang, Y. DARTS: Differentiable architecture search. In *International Conference on Learning Representations*, 2019.
- Marion, P. and Berthier, R. Leveraging the two timescale regime to demonstrate convergence of neural networks. In *Advances in Neural Information Processing Systems*, volume 36, 2023.
- Nichol, A. Q. and Dhariwal, P. Improved denoising diffusion probabilistic models. In Meila, M. and Zhang, T. (eds.), *Proceedings of the 38th International Conference on Machine Learning*, volume 139 of *Proceedings of Machine Learning Research*, pp. 8162–8171. PMLR, 18–24 Jul 2021.
- Nitanda, A. Stochastic proximal gradient descent with acceleration techniques. *Advances in Neural Information Processing Systems*, 27, 2014.
- Pachpatte, B. G. and Ames, W. *Inequalities for Differential and Integral Equations*. Elsevier, 1997.
- Papamakarios, G., Nalisnick, E., Rezende, D. J., Mohamed, S., and Lakshminarayanan, B. Normalizing flows for probabilistic modeling and inference. *The Journal of Machine Learning Research*, 22(1):2617–2680, 2021.
- Parisi, G. Correlation functions and computer simulations. *Nuclear Physics B*, 180(3):378–384, 1981.
- Pavliotis, G. A. *Stochastic processes and applications*. Springer, 2016.
- Pedregosa, F. Hyperparameter optimization with approximate gradient. In Balcan, M. F. and Weinberger, K. Q. (eds.), *Proceedings of The 33rd International Conference on Machine Learning*, volume 48 of *Proceedings of Machine Learning Research*, pp. 737–746, New York, New York, USA, 20–22 Jun 2016. PMLR.
- Pflug, G. C. *Optimization of Stochastic Models: the Interface between Simulation and Optimization*, volume 373. Springer Science & Business Media, 2012.
- Pontryagin, L. S. *Mathematical Theory of Optimal Processes*. Routledge, 1987.
- Protter, P. *Stochastic integration and differential equations. A new approach*, volume 21 of *Stochastic Modelling and Applied Probability*. Springer Berlin, Heidelberg, 2005.
- Roberts, G. O. and Tweedie, R. L. Exponential convergence of langevin distributions and their discrete approximations. *Bernoulli*, pp. 341–363, 1996.
- Ronneberger, O., Fischer, P., and Brox, T. U-net: Convolutional networks for biomedical image segmentation. In *Medical Image Computing and Computer-Assisted Intervention—MICCAI 2015: 18th International Conference, Munich, Germany, October 5-9, 2015, Proceedings, Part III 18*, pp. 234–241. Springer, 2015.
- Rosasco, L., Villa, S., and Vū, B. C. Convergence of stochastic proximal gradient algorithm. *Applied Mathematics & Optimization*, 82:891–917, 2020.
- Song, Y., Durkan, C., Murray, I., and Ermon, S. Maximum likelihood training of score-based diffusion models. *Advances in Neural Information Processing Systems*, 34: 1415–1428, 2021.
- Sutton, R. S., McAllester, D., Singh, S., and Mansour, Y. Policy gradient methods for reinforcement learning with function approximation. In *Advances in Neural Information Processing Systems*, volume 12, 1999.
- Tadić, V. B. and Doucet, A. Asymptotic bias of stochastic gradient search. *Annals of Applied Probability*, 27(6): 3255–3304, 2017.
- Tsybakov, A. *Introduction to nonparametric estimation*. Springer Series in Statistics. Springer, New York, 2009.

- Tzen, B. and Raginsky, M. Theoretical guarantees for sampling and inference in generative models with latent diffusions. In Beygelzimer, A. and Hsu, D. (eds.), *Proceedings of the Thirty-Second Conference on Learning Theory*, volume 99 of *Proceedings of Machine Learning Research*, pp. 3084–3114. PMLR, 25–28 Jun 2019.
- Vempala, S. and Wibisono, A. Rapid convergence of the unadjusted Langevin algorithm: Isoperimetry suffices. In *Advances in Neural Information Processing Systems*, volume 32, 2019.
- Vincent, P. A connection between score matching and denoising autoencoders. *Neural Computation*, 23(7):1661–1674, 2011.
- Wallace, B., Gokul, A., Ermon, S., and Naik, N. End-to-end diffusion latent optimization improves classifier guidance. *arXiv preprint arXiv:2303.13703*, 2023.
- Watson, D., Chan, W., Ho, J., and Norouzi, M. Learning fast samplers for diffusion models by differentiating through sample quality. In *International Conference on Learning Representations*, 2022.
- Wibisono, A. Sampling as optimization in the space of measures: The langevin dynamics as a composite optimization problem. In *Conference on Learning Theory*, pp. 2093–3027. PMLR, 2018.
- Williams, R. J. Simple statistical gradient-following algorithms for connectionist reinforcement learning. *Machine learning*, 8(3-4):229–256, 1992.
- Wu, X., Sun, K., Zhu, F., Zhao, R., and Li, H. Human preference score: Better aligning text-to-image models with human preference. In *Proceedings of the IEEE/CVF International Conference on Computer Vision (ICCV)*, pp. 2096–2105, October 2023.
- Xiao, L. and Zhang, T. A proximal stochastic gradient method with progressive variance reduction. *SIAM Journal on Optimization*, 24(4):2057–2075, 2014.
- Yang, J., Ji, K., and Liang, Y. Provably faster algorithms for bilevel optimization. *Advances in Neural Information Processing Systems*, 34:13670–13682, 2021.
- Ziegler, D. M., Stiennon, N., Wu, J., Brown, T. B., Radford, A., Amodei, D., Christiano, P., and Irving, G. Fine-tuning language models from human preferences. *arXiv preprint arXiv:1909.08593*, 2019.

Appendix

Organization of the Appendix. Section A is devoted to explanations on our methodology. Section A.1 gives precisions on the gradient estimation setting we consider. Then, in the case of Langevin dynamics (Section A.2), and denoising diffusions (Section A.3), we explain how Definition 3.1 and our Implicit Differentiation algorithms (Algorithms 2 and 3) can be instantiated in these cases. Section A.4 gives more details about the implicit differentiation approaches sketched in Section 3.2. Section B contains the proofs of our theoretical results, while Section C gives details for the experiments of Section 5 as well as additional explanations and plots. Finally, Section D is dedicated to additional related work.

A. Implicit Diffusion algorithms

A.1. Gradient estimation abstraction: Γ

As discussed in Section 3.1, we focus on settings where the gradient of the loss $\ell : \mathbb{R}^p \rightarrow \mathbb{R}$, defined by

$$\ell(\theta) := \mathcal{F}(\pi^*(\theta)),$$

can be estimated by using a function Γ . More precisely, following Definition 3.1, we assume that there exists a function $\Gamma : \mathcal{P} \times \mathbb{R}^p \rightarrow \mathbb{R}^p$ such that $\nabla \ell(\theta) = \Gamma(\pi^*(\theta), \theta)$. In practice, for almost every setting there is no closed form for $\pi^*(\theta)$, and even sampling from it can be challenging (e.g. here, if it is the outcome of infinitely many sampling steps). When we run our algorithms, the dynamic is in practice applied to variables, as discussed in Section 2.1. Using a batch of variables of size n , initialized independent with $X_0^i \sim p_0$, we have at each step k of joint sampling and optimization a batch of variables forming an empirical measure $\hat{p}_k^{(n)}$. We consider cases where the operator Γ is well-behaved: if $\hat{p}^{(n)} \approx p$, then $\Gamma(\hat{p}^{(n)}, \theta) = \Gamma(p, \theta)$, and therefore where this finite sample approximation can be used to produce an accurate estimate of $\nabla \ell(\theta)$.

A.2. Langevin dynamics

We explain how to derive the formulas (9)–(10) for Γ , and give the sample version of Algorithm 2 in these cases.

Recall that the stationary distribution of the dynamics (5) is the Gibbs distribution (6), with the normalization factor $Z_\theta = \int \exp(-V(x, \theta)) dx$. Assume that the outer objective writes as the expectation of some (potentially non-differentiable) reward R , namely $\mathcal{F}(p) := -\mathbb{E}_{x \sim p}[R(x)]$. Then our objective writes

$$\ell_{\text{reward}}(\theta) = - \int R(x) \frac{\exp(-V(x, \theta))}{Z_\theta} dx.$$

As a consequence,

$$\begin{aligned} \nabla \ell_{\text{reward}}(\theta) &= \int R(x) \nabla_2 V(x, \theta) \frac{\exp(-V(x, \theta))}{Z_\theta} dx - \int R(x) \frac{\exp(-V(x, \theta)) \int \nabla_2 V(x', \theta) \exp(-V(x', \theta)) dx'}{Z_\theta^2} dx \\ &= \mathbb{E}_{X \sim \pi^*(\theta)}[R(X) \nabla_2 V(X, \theta)] - \mathbb{E}_{X \sim \pi^*(\theta)}[R(X)] \mathbb{E}_{X \sim \pi^*(\theta)}[\nabla_2 V(X, \theta)] \\ &= \text{Cov}_{X \sim \pi^*(\theta)}[R(X), \nabla_2 V(X, \theta)]. \end{aligned}$$

This computation is sometimes referred to as the REINFORCE trick (Williams, 1992). This suggests taking

$$\Gamma_{\text{reward}}(p, \theta) = \text{Cov}_{X \sim p}[R(X), \nabla_2 V(X, \theta)].$$

In this case, the sample version of Algorithm 2 writes

$$\begin{aligned} X_{k+1}^{(i)} &= X_k^{(i)} - \gamma_X \nabla_1 V(X_k^{(i)}, \theta_k) + \sqrt{2\gamma_X} \Delta B_k^{(i)}, \quad \text{for all } i \in \{1, \dots, n\} \\ \theta_{k+1} &= \theta_k - \gamma_\theta \hat{\text{Cov}}[R(X_k^{(i)}), \nabla_2 V(X_k^{(i)}, \theta_k)], \end{aligned}$$

where $(\Delta B_k)_{k \geq 0}$ are i.i.d. standard Gaussian random variables and $\hat{\text{Cov}}$ is the empirical covariance over the sample.

When $\mathcal{F}(p) := \text{KL}(p_{\text{ref}} | p)$, e.g. when we want to stick or to regularize towards a reference distribution p_{ref} with sample access, for $\ell(\theta) = \mathcal{F}(\pi^*(\theta))$, we have

$$\ell_{\text{ref}}(\theta) = \int \log \left(\frac{p_{\text{ref}}[x]}{\pi^*(\theta)[x]} \right) p_{\text{ref}}[x] dx,$$

thus

$$\nabla \ell_{\text{ref}}(\theta) = - \int \frac{\partial \pi^*(\theta_t)}{\partial \theta} [x] \cdot \frac{1}{\pi^*(\theta)[x]} p_{\text{ref}}[x] dx.$$

Leveraging the explicit formula (6) for $\pi^*(\theta)$, we obtain

$$\begin{aligned} \nabla \ell_{\text{ref}}(\theta) &= \int \frac{\nabla_2 V(x, \theta) \exp(-V(x, \theta))}{\pi^*(\theta)[x] Z_\theta} p_{\text{ref}}[x] dx + \int \frac{\exp(-V(x, \theta)) \nabla_\theta Z_\theta}{\pi^*(\theta)[x] Z_\theta^2} p_{\text{ref}}[x] dx \\ &= \int \nabla_2 V(x, \theta) p_{\text{ref}}[x] dx + \int \frac{\nabla_\theta Z_\theta}{Z_\theta} p_{\text{ref}}[x] dx \\ &= \mathbb{E}_{X \sim p_{\text{ref}}}[\nabla_2 V(X, \theta)] - \int \nabla_2 V(x, \theta) \frac{\exp(-V(x, \theta))}{Z_\theta} dx \\ &= \mathbb{E}_{X \sim p_{\text{ref}}}[\nabla_2 V(X, \theta)] - \mathbb{E}_{X \sim \pi^*(\theta)}[\nabla_2 V(X, \theta)], \end{aligned}$$

where the third equality uses that $\int p_{\text{ref}}[x] dx = 1$. This suggests taking

$$\Gamma_{\text{ref}}(p, \theta) = \mathbb{E}_{X \sim p}[\nabla_2 V(X, \theta)] - \mathbb{E}_{X \sim \pi^*(\theta)}[\nabla_2 V(X, \theta)].$$

The terms in this gradient can be estimated: for a model $V(\cdot, \theta)$, the gradient function w.r.t θ can be obtained by automatic differentiation. Samples from p_{ref} are available by assumption, and samples from $\pi^*(\theta)$ can be replaced by the X_k in joint optimization as above. We recover the formula for contrastive learning of energy-based model to data from p_{ref} (Gutmann & Hyvärinen, 2012).

This can also be used for finetuning, combining a reward R and a KL term, with $\mathcal{F}(p) = -\lambda \mathbb{E}_{X \sim p}[R(x)] + \beta \text{KL}(p || p_{\text{ref}})$. The sample version of Algorithm 2 then writes

$$\begin{aligned} X_{k+1}^{(i)} &= X_k^{(i)} - \gamma_X \nabla_1 V(X_k^{(i)}, \theta_k) + \sqrt{2\gamma_X} \Delta B_k^{(i)} \quad \text{for all } i \in \{1, \dots, n\} \\ \theta_{k+1} &= \theta_k - \gamma_\theta \left[\hat{\lambda} \text{Cov}[R(X_k), \nabla_2 V(X_k, \theta_k)] + \beta \left(\sum_{j=1}^m \nabla_2 V(\tilde{X}_k^{(j)}, \theta) - \frac{1}{n} \sum_{i=1}^n \nabla_2 V(X_k^{(i)}, \theta) \right) \right], \end{aligned}$$

where $(\Delta B_k)_{k \geq 0}$ are i.i.d. standard Gaussian random variables, $\hat{\text{Cov}}$ is the empirical covariance over the sample, and $\tilde{X}_k^{(j)} \sim p_{\text{ref}}$.

A.3. Adjoint method and denoising diffusions

We explain how to use the adjoint method to backpropagate through differential equations, and apply this to derive instantiations of Algorithm 3 for denoising diffusions.

ODE sampling. We begin by recalling the adjoint method in the ODE case (Pontryagin, 1987). Consider the ODE $dY_t = \mu(t, Y_t, \theta) dt$ integrated between 0 and some $T > 0$. For some differentiable function $R : \mathbb{R}^d \rightarrow \mathbb{R}$, the derivative of $R(Y_T)$ with respect to θ can be computed by the adjoint method. More precisely, it is equal to G_T defined by

$$\begin{aligned} Z_0 &= Y_T, & dZ_t &= -\mu(t, Z_t, \theta) dt, \\ A_0 &= \nabla R(Y_T), & dA_t &= A_t^\top \nabla_2 \mu(T-t, Z_t, \theta) dt, \\ G_0 &= 0, & dG_t &= A_t^\top \nabla_3 \mu(T-t, Z_t, \theta) dt. \end{aligned}$$

Note that sometimes the adjoint equations are written with a reversed time index ($t' = T - t$), which is not the formalism we adopt here.

In the setting of denoising diffusion presented in Section 2.2, we are not interested in computing the derivative of a function of a single realization of the ODE, but of the expectation over $Y_T \sim \pi^*(\theta)$ of the derivative of $R(Y_T)$ with respect to θ . In other words, we want to compute $\nabla \ell(\theta) = \nabla(\mathcal{F} \circ \pi^*)(\theta)$, where $\mathcal{F}(p) = \mathbb{E}_{x \sim p}[R(x)]$. Rewriting the equations above in this case, we obtain that G_T defined by

$$\begin{aligned} Z_0 &\sim \pi^*(\theta), & dZ_t &= -\mu(t, Z_t, \theta) dt, \\ A_0 &= \nabla R(Z_0), & dA_t &= A_t^\top \nabla_2 \mu(T-t, Z_t, \theta) dt, \\ G_0 &= 0, & dG_t &= A_t^\top \nabla_3 \mu(T-t, Z_t, \theta) dt \end{aligned}$$

is an unbiased estimator of $\nabla \ell(\theta)$. Recalling Definition 3.1, this means that we can take $\Gamma(p, \theta) := G_T$ defined by

$$\begin{aligned} Z_0 &\sim p, & dZ_t &= -\mu(t, Z_t, \theta)dt \\ A_0 &= \nabla R(Z_0), & dA_t &= A_t^\top \nabla_2 \mu(T-t, Z_t, \theta)dt \\ G_0 &= 0, & dG_t &= A_t^\top \nabla_3 \mu(T-t, Z_t, \theta)dt. \end{aligned}$$

This is exactly the definition of Γ given in Section 3.2. We apply this to the case of denoising diffusions, where μ is given by (8). To avoid a notation clash between the number of iterations $T = M$ of the sampling algorithm, and the maximum time T of the ODE in (8), we rename the latter to T_{horizon} . A direct instantiation of Algorithm 3 with an Euler solver is the following algorithm.

Algorithm 4 Implicit Diff. optimization, denoising diffusions with ODE sampling

input $\theta_0 \in \mathbb{R}^p, p_0 \in \mathcal{P}$
input $P_M = [Y_0^{(0)}, \dots, Y_0^{(M)}] \sim \mathcal{N}(0, 1)^{\otimes (m \times d)}$
for $k \in \{0, \dots, K-1\}$ **do**
 $Y_{k+1}^{(0)} \sim \mathcal{N}(0, 1)$
parallel $Y_{k+1}^{(m+1)} \leftarrow Y_k^{(m)} + \frac{1}{M} \mu(\frac{mT_{\text{horizon}}}{M}, Y_k^{(m)}, \theta_k)$ **for** $m \in [M-1]$
 $Z_k^{(0)} \leftarrow Y_k^{(M)}$
 $A_k^{(0)} \leftarrow \nabla R(Z_k^{(0)})$
 $G_k^{(0)} \leftarrow 0$
for $t \in \{0, \dots, T-1\}$ **do**
 $Z_k^{(t+1)} \leftarrow Z_k^{(t)} - \frac{1}{T} \mu(\frac{tT_{\text{horizon}}}{T}, Z_k^{(t)}, \theta_k)$
 $A_k^{(t+1)} \leftarrow A_k^{(t)} + \frac{1}{T} (A_k^{(t)})^\top \nabla_2 \mu(\frac{tT_{\text{horizon}}}{T}, Z_k^{(t)}, \theta_k)$
 $G_k^{(t+1)} \leftarrow G_k^{(t)} + \frac{1}{T} (G_k^{(t)})^\top \nabla_2 \mu(\frac{tT_{\text{horizon}}}{T}, Z_k^{(t)}, \theta_k)$
 $\theta_{k+1} \leftarrow \theta_k - \eta G_k^{(T)}$
output θ_K

Several comments are in order. First, the dynamics of $Y_k^{(M)}$ in the previous M steps, from $Y_{k-M}^{(0)}$ to $Y_{k-1}^{(M-1)}$, uses the M previous values of the parameter $\theta_{k-M}, \dots, \theta_{k-1}$. This means that $Y_k^{(M)}$ does not correspond to the result of sampling with any given parameter θ , since we are at the same time performing the sampling process and updating θ .

Besides, the computation of $\Gamma(p, \theta)$ is the outcome of an iterative process, namely calling an ODE solver. Therefore, it is also possible to use the same queuing trick as for sampling iterations to decrease the cost of this step by leveraging parallelization. For completeness, the variant is given below.

Algorithm 5 Implicit Diff. optimization, denoising diffusions with ODE sampling, variant with a double queue

input $\theta_0 \in \mathbb{R}^p, p_0 \in \mathcal{P}$
input $P_M = [Y_0^{(0)}, \dots, Y_0^{(M)}] \sim \mathcal{N}(0, 1)^{\otimes (m \times d)}$
for $k \in \{0, \dots, K-1\}$ (joint single loop) **do**
 $Y_{k+1}^{(0)} \sim \mathcal{N}(0, 1)$
 $Z_{k+1}^{(0)} \leftarrow Y_k^{(M)}$
 $A_{k+1}^{(0)} \leftarrow \nabla R(Z_{k+1}^{(0)})$
 $G_{k+1}^{(0)} \leftarrow 0$
parallel $Y_{k+1}^{(m+1)} \leftarrow Y_k^{(m)} + \frac{1}{M} \mu(\frac{mT_{\text{horizon}}}{M}, Y_k^{(m)}, \theta_k)$ **for** $m \in [M-1]$
parallel $Z_{k+1}^{(m+1)} \leftarrow Z_k^{(m)} - \frac{1}{M} \mu(\frac{mT_{\text{horizon}}}{M}, Z_k^{(m)}, \theta_k)$ **for** $m \in [M-1]$
parallel $A_{k+1}^{(m+1)} \leftarrow A_k^{(m)} + \frac{1}{M} (A_k^{(m)})^\top \nabla_2 \mu(\frac{mT_{\text{horizon}}}{M}, Z_k^{(m)}, \theta_k)$ **for** $m \in [M-1]$
parallel $G_{k+1}^{(m+1)} \leftarrow G_k^{(m)} + \frac{1}{M} (G_k^{(m)})^\top \nabla_2 \mu(\frac{mT_{\text{horizon}}}{M}, Z_k^{(m)}, \theta_k)$ **for** $m \in [M-1]$
 $\theta_{k+1} \leftarrow \theta_k - \eta G_k^{(M)}$
output θ_K

Second, each variable $Y_k^{(m)}$ consists of a single sample of \mathbb{R}^d . The algorithm straightforwardly extends when each variable $Y_k^{(m)}$ is a batch of samples. Finally, we consider so far the case where the size of the queue M is equal to the number of sampling steps T . We give below the variant of Algorithm 4 when $M \neq T$ but M divides T . Taking M from 1 to T balances between a single-loop and a nested-loop algorithm.

Algorithm 6 Implicit Diff. optimization, denoising diffusions with ODE sampling, $M \neq T$, M divides T

input $\theta_0 \in \mathbb{R}^p, p_0 \in \mathcal{P}$
input $P_M = [Y_0^{(0)}, \dots, Y_0^{(M)}] \sim \mathcal{N}(0, 1)^{\otimes (m \times d)}$
for $k \in \{0, \dots, K-1\}$ **do**
 $Y_{k+1}^{(0)} \sim \mathcal{N}(0, 1)$
parallel $Y_{k+1/2}^{(m+1)} \leftarrow Y_k^{(m)}$ for $m \in [M-1]$
for $t \in \{0, \dots, T/M-1\}$ **in parallel for** $m \in [M-1]$ **do**
 $Y_{k+1/2}^{(m+1)} \leftarrow Y_{k+1/2}^{(m)} + \frac{1}{T} \mu\left(\left(\frac{m}{M} + \frac{t}{T}\right)T_{\text{horizon}}, Y_{k+1/2}^{(m)}, \theta_k\right)$
parallel $Y_{k+1}^{(m+1)} \leftarrow Y_{k+1/2}^{(m+1)}$ for $m \in [M-1]$
 $Z_k^{(0)} \leftarrow Y_k^{(M)}$
 $A_k^{(0)} \leftarrow \nabla R(Z_k^{(0)})$
 $G_k^{(0)} \leftarrow 0$
for $t \in \{0, \dots, T-1\}$ **do**
 $Z_k^{(t+1)} \leftarrow Z_k^{(t)} - \frac{1}{T} \mu\left(\frac{tT_{\text{horizon}}}{T}, Z_k^{(t)}, \theta_k\right)$
 $A_k^{(t+1)} \leftarrow A_k^{(t)} + \frac{1}{T} (A_k^{(t)})^\top \nabla_2 \mu\left(\frac{tT_{\text{horizon}}}{T}, Z_k^{(t)}, \theta_k\right)$
 $G_k^{(t+1)} \leftarrow G_k^{(t)} + \frac{1}{T} (G_k^{(t)})^\top \nabla_2 \mu\left(\frac{tT_{\text{horizon}}}{T}, Z_k^{(t)}, \theta_k\right)$
 $\theta_{k+1} \leftarrow \theta_k - \eta G_k^{(T)}$
output θ_K

Algorithm 5 extends to this case similarly.

SDE sampling. The adjoint method is also defined in the SDE case (Li et al., 2020). Consider the SDE

$$dY_t = \mu(t, Y_t, \theta)dt + \sqrt{2}dB_t, \quad (15)$$

integrated between 0 and some $T > 0$. This setting encompasses the denoising diffusion SDE (7) with the appropriate choice of μ . For some differentiable function $R : \mathbb{R}^d \rightarrow \mathbb{R}$ and for a given realization $(Y_t)_{0 \leq t \leq T}$ of the SDE, the derivative of $R(Y_T)$ with respect to θ is equal to G_T defined by

$$\begin{aligned} A_0 &= \nabla R(Y_T), & dA_t &= A_t^\top \nabla_2 \mu(T-t, Y_{T-t}, \theta)dt, \\ G_0 &= 0, & dG_t &= A_t^\top \nabla_3 \mu(T-t, Y_{T-t}, \theta)dt. \end{aligned} \quad (16)$$

This is a similar equation as in the ODE case. The main difference is that it is not possible to recover Y_{T-t} only from the terminal value of the path Y_T , but that we need to keep track of the randomness from the Brownian motion B_t . Efficient ways to do so are presented in Li et al. (2020); Kidger et al. (2021). In a nutshell, they consist in only keeping in memory the seed used to generate the Brownian motion, and recomputing the path from the seed.

Using the SDE sampler allows to incorporate a KL term in the reward. Indeed, consider the SDE (15) for two different parameters θ_1 and θ_2 , with associated variables Y_t^1 and Y_t^2 . Then, by Girsanov's theorem (see Protter, 2005, Chapter III.8, and Tzen & Raginsky, 2019 for use in a similar context), the KL divergence between the paths Y_t^1 and Y_t^2 is

$$\text{KL}((Y_t^1)_{t \geq 0} \parallel (Y_t^2)_{t \geq 0}) = \int_0^T \mathbb{E}_{y \sim q_t^1} \|\mu(t, y, \theta_1) - \mu(t, y, \theta_2)\|^2 dt, \quad (17)$$

where q_t^1 denotes the distribution of Y_t^1 . This term can be (stochastically) estimated at the same time as the SDE (15) is simulated, by appending a new coordinate to Y_t (and to μ) that integrates (17) over time. Then, adding the KL in the reward

is as simple as adding a linear term in $\tilde{R} : \mathbb{R}^{d+1} \rightarrow \mathbb{R}$, that is, $\tilde{R}(x) = R(x[: -1]) + x[-1]$ (using Numpy notation, where ‘-1’ denotes the last index). The same idea is used in [Dvijotham et al. \(2023\)](#) to incorporate a KL term in reward finetuning of denoising diffusion models.

A.4. Implicit differentiation

Finite dimension. Take $g : \mathbb{R}^m \times \mathbb{R}^p \rightarrow \mathbb{R}$ a continuously differentiable function. Then $x^*(\theta) = \operatorname{argmin} g(\cdot, \theta)$ implies a stationary point condition $\nabla_1 g(x^*(\theta_0), \theta_0) = 0$. In this case, it is possible to define and analyze the function $x^* : \mathbb{R}^p \rightarrow \mathbb{R}^m$ and its variations. Note that this generalizes to the case where $x^*(\theta)$ can be written as the root of a parameterized system.

More precisely, the **implicit function theorem** (see, e.g., [Griewank & Walther, 2008](#); [Krantz & Parks, 2002](#), and references therein) can be applied. Under differentiability assumptions on g , for (x_0, θ_0) such that $\nabla_1 g(x_0, \theta_0) = 0$ with a continuously differentiable $\nabla_1 g$, and if the Hessian $\nabla_{1,1}^2 g$ evaluated at (x_0, θ_0) is a square invertible matrix, then there exists a function $x^*(\cdot)$ over a neighborhood of θ_0 satisfying $x^*(\theta_0) = x_0$. Furthermore, for all θ in this neighborhood, we have that $\nabla_1 g(x^*(\theta), \theta) = 0$ and its Jacobian $\partial x^*(\theta)$ exists. It is then possible to differentiate with respect to θ both sides of the equation $\nabla_1 g(x^*(\theta), \theta) = 0$, which yields a linear equation satisfied by this Jacobian

$$\nabla_{1,1} g(x^*(\theta_0), \theta_0) \partial x^*(\theta) + \nabla_{1,2} g(x^*(\theta_0), \theta_0) = 0.$$

This formula can be used for automatic implicit differentiation, when both the evaluation of the derivatives in this equation and the inversion of the linear system can be done automatically ([Blondel et al., 2022](#)).

Extension to space of probabilities. When $\mathcal{G} : \mathcal{P} \times \mathbb{R}^p \rightarrow \mathbb{R}$ and $\pi^*(\theta) = \operatorname{argmin} \mathcal{G}(\cdot, \theta)$ as in (3), under assumptions on differentiability and uniqueness of the solution on \mathcal{G} , this can also be extended to a distribution setting. We write here the infinite-dimensional equivalent of the above equations, involving derivatives or variations over the space of probabilities, and refer to [Ambrosio et al. \(2005\)](#) for more details.

First, we have that

$$\nabla \ell(\theta) = \nabla_\theta (\mathcal{F}(\pi^*(\theta))) = \int \mathcal{F}'(p)[x] \nabla_\theta \pi^*(\theta)[x] dx,$$

where $\mathcal{F}'(p) : \mathcal{X} \rightarrow \mathbb{R}$ denotes the first variation of \mathcal{F} at $p \in \mathcal{P}$ (see Definition B.1). This yields $\nabla \ell(\theta) = \Gamma(\pi^*(\theta), \theta)$ with

$$\Gamma(p, \theta) = \int \mathcal{F}'(p)[x] \gamma(p, \theta)[x] dx.$$

where $\gamma(p, \theta)$ is the solution of the linear system

$$\int \nabla_{1,1} \mathcal{G}(p, \theta)[x, x'] \gamma(p, \theta)[x'] dx' = -\nabla_{1,2} \mathcal{G}(p, \theta)[x],$$

Although this gives us a general way to define gradients of $\pi^*(\theta)$ with respect to θ , solving this linear system is generally not feasible. One exception is when sampling over a finite state space \mathcal{X} , in which case \mathcal{P} is finite-dimensional, and the integrals boil down to matrix-vector products.

B. Theoretical analysis

B.1. Langevin with continuous flow

B.1.1. ADDITIONAL DEFINITIONS

Notations. We denote by $\mathcal{P}_2(\mathbb{R}^d)$ the set of probability measures on \mathbb{R}^d with bounded second moments. Given a Lebesgue measurable map $T : X \rightarrow X$ and $\mu \in \mathcal{P}_2(X)$, $T_\# \mu$ is the pushforward measure of μ by T . For any $\mu \in \mathcal{P}_2(\mathbb{R}^d)$, $L^2(\mu)$ is the space of functions $f : \mathbb{R}^d \rightarrow \mathbb{R}$ such that $\int \|f\|^2 d\mu < \infty$. We denote by $\|\cdot\|_{L^2(\mu)}$ and $\langle \cdot, \cdot \rangle_{L^2(\mu)}$ respectively the norm and the inner product of the Hilbert space $L^2(\mu)$. We consider, for $\mu, \nu \in \mathcal{P}_2(\mathbb{R}^d)$, the 2-Wasserstein distance $W_2(\mu, \nu) = \inf_{s \in \mathcal{S}(\mu, \nu)} \int \|x - y\|^2 ds(x, y)$, where $\mathcal{S}(\mu, \nu)$ is the set of couplings between μ and ν . The metric space $(\mathcal{P}_2(\mathbb{R}^d), W_2)$ is called the Wasserstein space.

Let $\mathcal{F} : \mathcal{P}(\mathbb{R}^d) \rightarrow \mathbb{R}^+$ a functional.

Definition B.1. If it exists, the *first variation of \mathcal{F} at ν* is the function $\mathcal{F}'(\nu) : \mathbb{R}^d \rightarrow \mathbb{R}$ s. t. for any $\mu \in \mathcal{P}(\mathbb{R}^d)$, with $\xi = \mu - \nu$:

$$\lim_{\epsilon \rightarrow 0} \frac{1}{\epsilon} (\mathcal{F}(\nu + \epsilon\xi) - \mathcal{F}(\nu)) = \int_{\mathbb{R}^d} \mathcal{F}'(\nu)(x) d\xi(x),$$

and is defined uniquely up to an additive constant.

We will extensively apply the following formula:

$$\frac{d\mathcal{F}(p_t)}{dt} = \int \mathcal{F}'(p_t) \frac{\partial p_t}{\partial t} = \int \mathcal{F}'(p_t)[x] \frac{\partial p_t[x]}{\partial t} dx. \quad (18)$$

We will also rely regularly on the definition of a Wasserstein gradient flow, since Langevin dynamics correspond to a Wasserstein gradient flow of the Kullback-Leibler (KL) divergence (Jordan et al., 1998; Wibisono, 2018). A Wasserstein gradient flow of \mathcal{F} (Ambrosio et al., 2005) can be described by the following continuity equation:

$$\frac{\partial \mu_t}{\partial t} = \nabla \cdot (\mu_t \nabla_{W_2} \mathcal{F}(\mu_t)), \quad \nabla_{W_2} \mathcal{F}(\mu_t) = \nabla \mathcal{F}'(\mu_t), \quad (19)$$

where \mathcal{F}' denotes the first variation. Equation (19) holds in the sense of distributions (i.e. the equation above holds when integrated against a smooth function with compact support), see Ambrosio et al. (2005, Chapter 8). In particular, if $\mathcal{F} = \text{KL}(\cdot|\pi)$ for $\pi \in \mathcal{P}_2(\mathbb{R}^d)$, then $\nabla_{W_2} \mathcal{F}(\mu) = \nabla \log(\mu/\pi)$. In this case, the corresponding continuity equation is known as the Fokker-Planck equation, and in particular it is known that the law p_t of Langevin dynamics:

$$dX_t = \nabla \log(\pi(X_t))dt + \sqrt{2}dB_t$$

satisfies the Fokker-Planck equation (Pavliotis, 2016, Chapter 3).

B.1.2. GAUSSIAN MIXTURES SATISFY THE ASSUMPTIONS

We begin by a more formal statement of the result stated in Section 4.1.

Proposition B.2. *Let*

$$V(x, \theta) := -\log \left(\sum_{i=1}^p H(\theta_i) \exp(-\|x - z_i\|^2) \right),$$

for some fixed $z_1, \dots, z_p \in \mathbb{R}^d$ and where

$$H(x) := \eta + (1 - \eta) \cdot \frac{1}{1 + e^{-x}}$$

is a shifted version of the logistic function for some $\eta \in (0, 1)$. Then Assumptions 4.1 and 4.2 hold.

Proof. Assumption 4.1 holds since a mixture of Gaussians is Log-Sobolev with a bounded constant (Chen et al., 2021a, Corollary 1). Note that the constant deteriorates as the modes of the mixture get further apart.

Furthermore, Assumption 4.2 holds since, for all $\theta \in \mathbb{R}^p$ and $x \in \mathbb{R}^d$,

$$\|\nabla_2 V(x, \theta)\|_1 = \frac{\sum_{i=1}^p H'(\theta_i) \exp(-\|x - z_i\|^2)}{\sum_{i=1}^p H(\theta_i) \exp(-\|x - z_i\|^2)} \leq \frac{\sum_{i=1}^p \exp(-\|x - z_i\|^2)}{\sum_{i=1}^p \eta \exp(-\|x - z_i\|^2)} \leq \frac{1}{\eta}.$$

□

B.1.3. PROOF OF PROPOSITION 4.4

In the case of the functions Γ defined by (9)–(10), we see that Γ is bounded under Assumption 4.2 and when the reward R is bounded. The Lipschitz continuity can be obtained as follows. Consider for instance the case of (10) where $\Gamma(p, \theta)$ is given by

$$\Gamma_{\text{ref}}(p, \theta) = \mathbb{E}_{X \sim p_{\text{ref}}}[\nabla_2 V(X, \theta)] - \mathbb{E}_{X \sim p}[\nabla_2 V(X, \theta)].$$

Then

$$\begin{aligned} \|\Gamma_{\text{ref}}(p, \theta) - \Gamma_{\text{ref}}(q, \theta)\| &= \|\mathbb{E}_{X \sim q}[\nabla_2 V(X, \theta)] - \mathbb{E}_{X \sim p}[\nabla_2 V(X, \theta)]\| \\ &\leq C \text{TV}(p, q) \\ &\leq \frac{C}{\sqrt{2}} \sqrt{\text{KL}(p \| q)}, \end{aligned}$$

where the first inequality comes from the fact that the total variation distance is an integral probability metric generated by the set of bounded functions, and the second inequality is Pinsker's inequality (Tsybakov, 2009, Lemma 2.5). The first case of Section A.2 unfolds similarly.

B.1.4. PROOF OF THEOREM 4.5

The dynamics (11)–(12) can be rewritten equivalently on $\mathcal{P}_2(\mathbb{R}^d)$ and \mathbb{R}^p as

$$\frac{\partial p_t}{\partial t} = \nabla \cdot (p_t \nabla_{W_2} \mathcal{G}(p_t, \theta_t)) \quad (20)$$

$$d\theta_t = -\varepsilon_t \Gamma(p_t, \theta_t) dt, \quad (21)$$

where $\mathcal{G}(p, \theta) = \text{KL}(p \| \pi_\theta^*)$, see Appendix B.1.1. The Wasserstein gradient in (20) is taken with respect to the first variable of \mathcal{G} .

Evolution of the loss. Recall that Γ satisfies by Definition 3.1 that $\nabla \ell(\theta) = \Gamma(\pi^*(\theta), \theta)$. Thus we have, by (21),

$$\begin{aligned} \frac{d\ell}{dt}(t) &= \left\langle \nabla \ell(\theta_t), \frac{d\theta_t}{dt} \right\rangle \\ &= -\varepsilon_t \langle \nabla \ell(\theta_t), \Gamma(p_t, \theta_t) \rangle \\ &= -\varepsilon_t \langle \nabla \ell(\theta_t), \Gamma(\pi^*(\theta_t), \theta_t) \rangle + \varepsilon_t \langle \nabla \ell(\theta_t), \Gamma(\pi^*(\theta_t), \theta_t) - \Gamma(p_t, \theta_t) \rangle \\ &\leq -\varepsilon_t \|\nabla \ell(\theta_t)\|^2 + \varepsilon_t \|\nabla \ell(\theta_t)\| \|\Gamma(\pi^*(\theta_t), \theta_t) - \Gamma(p_t, \theta_t)\|. \end{aligned}$$

Then, by Assumption 4.3,

$$\frac{d\ell}{dt}(t) \leq -\varepsilon_t \|\nabla \ell(\theta_t)\|^2 + \varepsilon_t K_\Gamma \|\nabla \ell(\theta_t)\| \sqrt{\text{KL}(p_t \| \pi^*(\theta_t))}.$$

Using $ab \leq \frac{1}{2}(a^2 + b^2)$, we get

$$\frac{d\ell}{dt}(t) \leq -\frac{1}{2}\varepsilon_t \|\nabla \ell(\theta_t)\|^2 + \frac{1}{2}\varepsilon_t K_\Gamma^2 \text{KL}(p_t \| \pi^*(\theta_t)), \quad (22)$$

Bounding the KL divergence of p_t from $\pi^*(\theta_t)$. Recall that

$$\text{KL}(p_t \| \pi^*(\theta_t)) = \int \log \left(\frac{p_t}{\pi^*(\theta_t)} \right) p_t.$$

Thus, by the chain rule formula (18),

$$\frac{d \text{KL}(p_t \| \pi^*(\theta_t))}{dt} = \int \log \left(\frac{p_t}{\pi^*(\theta_t)} \right) \frac{\partial p_t}{\partial t} + \int \frac{p_t}{\pi^*(\theta_t)} \frac{\partial \pi^*(\theta_t)}{\partial t} := a + b.$$

From an integration by parts, using (20) and by Assumption 4.1, we have

$$\begin{aligned} a &= \int \log \left(\frac{p_t}{\pi^*(\theta_t)} \right) \frac{\partial p_t}{\partial t} = \int \log \left(\frac{p_t}{\pi^*(\theta_t)} \right) \nabla \cdot \left(p_t \nabla \log \left(\frac{p_t}{\pi^*(\theta_t)} \right) \right) \\ &= \left\langle \nabla \log \left(\frac{p_t}{\pi^*(\theta_t)} \right), -\nabla \log \left(\frac{p_t}{\pi^*(\theta_t)} \right) \right\rangle_{L^2(p_t)} = - \left\| \nabla \log \left(\frac{p_t}{\pi^*(\theta_t)} \right) \right\|_{L^2(p_t)}^2 \leq -2\mu \text{KL}(p_t \| \pi^*(\theta_t)). \end{aligned}$$

Moving on to b , we have

$$b = \int \frac{p_t}{\pi^*(\theta_t)} \frac{\partial \pi^*(\theta_t)}{\partial t} = \int p_t \frac{\partial \log(\pi^*(\theta_t))}{\partial t}.$$

By the chain rule and (21), we have for $x \in \mathcal{X}$

$$\frac{\partial \pi^*(\theta_t)}{\partial t}[x] = \left\langle \frac{\partial \pi^*(\theta_t)}{\partial \theta}[x], \frac{d\theta_t}{dt} \right\rangle = \left\langle \frac{\partial \pi^*(\theta_t)}{\partial \theta}[x], -\varepsilon_t \Gamma(p_t, \theta_t) \right\rangle.$$

Using $\pi^*(\theta) \propto e^{-V(\theta, \cdot)}$ (with similar computations as for $\nabla \ell_{\text{ref}}$ in Section A.2), we have

$$\frac{\partial \pi^*(\theta_t)}{\partial t}[x] = \left\langle -\nabla_2 V(x, \theta_t) \pi^*(\theta_t)[x] + \mathbb{E}_{X \sim \pi^*(\theta_t)}(\nabla_2 V(X, \theta_t)) \pi^*(\theta_t)[x], -\varepsilon_t \Gamma(p_t, \theta_t) \right\rangle,$$

and

$$\frac{\partial \log(\pi^*(\theta_t))}{\partial t} = \varepsilon_t \langle \nabla_2 V(\cdot, \theta_t) - \mathbb{E}_{X \sim \pi^*(\theta_t)}(\nabla_2 V(X, \theta_t)), \Gamma(p_t, \theta_t) \rangle.$$

This yields

$$\begin{aligned} b &= \varepsilon_t \int \langle \nabla_2 V(x, \theta_t) - \mathbb{E}_{X \sim \pi^*(\theta_t)}(\nabla_2 V(X, \theta_t)), \Gamma(p_t, \theta_t) \rangle p_t[x] dx \\ &= \varepsilon_t \left\langle \int \nabla_2 V(x, \theta_t) dp_t[x] - \mathbb{E}_{X \sim \pi^*(\theta_t)}(\nabla_2 V(X, \theta_t)), \Gamma(p_t, \theta_t) \right\rangle \\ &\leq \varepsilon_t \|\Gamma(p_t, \theta_t)\|_{\mathbb{R}^p} (\|\nabla_2 V(\cdot, \theta_t)\|_{L^2(p_t)} + \|\nabla_2 V(\cdot, \theta_t)\|_{L^2(\pi^*(\theta_t))}) \\ &\leq 2C^2 \varepsilon_t, \end{aligned}$$

where the last step uses Assumptions 4.2 and 4.3. Putting everything together, we obtain

$$\frac{d \text{KL}(p_t \parallel \pi^*(\theta_t))}{dt} \leq -2\mu \text{KL}(p_t \parallel \pi^*(\theta_t)) + 2C^2 \varepsilon_t.$$

Using Grönwall's inequality (Pachpatte & Ames, 1997) to integrate the inequality, the KL divergence can be bounded by

$$\text{KL}(p_t \parallel \pi^*(\theta_t)) \leq \text{KL}(p_0 \parallel \pi^*(\theta_0)) e^{-2\mu t} + 2C^2 \int_0^t \varepsilon_s e^{2\mu(s-t)} ds.$$

Coming back to (22), we get

$$\frac{d\ell}{dt}(t) \leq -\frac{1}{2} \varepsilon_t \|\nabla \ell(\theta_t)\|^2 + \frac{1}{2} \varepsilon_t K_\Gamma^2 \left(\text{KL}(p_0 \parallel \pi^*(\theta_0)) e^{-2\mu t} + 2C^2 \int_0^t \varepsilon_s e^{2\mu(s-t)} ds \right).$$

Integrating between 0 and T , we have

$$\ell(T) - \ell(0) \leq -\frac{1}{2} \int_0^T \varepsilon_t \|\nabla \ell(\theta_t)\|^2 dt + \frac{K_\Gamma^2 \text{KL}(p_0 \parallel \pi^*(\theta_0))}{2} \int_0^T \varepsilon_t e^{-2\mu t} dt + K_\Gamma^2 C^2 \int_0^T \int_0^t \varepsilon_t \varepsilon_s e^{2\mu(s-t)} ds dt.$$

Since ε_t is decreasing, we can bound ε_t by ε_T in the first integral and rearrange terms to obtain

$$\frac{1}{T} \int_0^T \|\nabla \ell(\theta_t)\|^2 dt \leq \frac{2}{T \varepsilon_T} (\ell(0) - \inf \ell) + \frac{K_\Gamma^2 \text{KL}(p_0 \parallel \pi^*(\theta_0))}{T \varepsilon_T} \int_0^T \varepsilon_t e^{-2\mu t} dt + \frac{2K_\Gamma^2 C^2}{T \varepsilon_T} \int_0^T \int_0^t \varepsilon_t \varepsilon_s e^{2\mu(s-t)} ds dt. \quad (23)$$

Recall that, by assumption of the Theorem, $\varepsilon_t = \min(1, \frac{1}{\sqrt{t}})$. Thus $T \varepsilon_T = \sqrt{T}$, and the first term is bounded by a constant times $T^{-1/2}$. It is also the case of the second term since $\int_0^T \varepsilon_t e^{-2\mu t} dt$ is converging. Let us now estimate the magnitude of the last term. Let $T_0 \geq 2$ (depending only on μ) such that $\frac{\ln(T_0)}{2\mu} \leq \frac{T_0}{2}$. For $t \geq T_0$, let $\alpha(t) := t - \frac{\ln t}{2\mu}$. We have, for

$t \geq T_0$,

$$\begin{aligned} \int_0^t \varepsilon_s e^{2\mu(s-t)} ds &= \int_0^{\alpha(t)} \varepsilon_s e^{2\mu(s-t)} ds + \int_{\alpha(t)}^t \varepsilon_s e^{2\mu(s-t)} ds \\ &\leq \varepsilon_0 e^{-2\mu t} \int_0^{\alpha(t)} e^{2\mu s} ds + (t - \alpha(t)) \varepsilon_{\alpha(t)} \\ &\leq \frac{\varepsilon_0}{2\mu} e^{2\mu(\alpha(t)-t)} + \frac{\varepsilon_{\alpha(t)} \ln t}{2\mu} \\ &\leq \frac{\varepsilon_0}{2\mu t} + \frac{\varepsilon_{t/2} \ln t}{2\mu}, \end{aligned}$$

where in the last inequality we used that $\alpha(t) \geq t/2$ and ε_t is decreasing. For $t < T_0$, we can simply bound the integral $\int_0^t \varepsilon_s e^{\mu(s-t)} ds$ by $\varepsilon_0 T_0$. We obtain

$$\int_0^T \int_0^t \varepsilon_t \varepsilon_s e^{2\mu(s-t)} ds \leq \int_0^{T_0} \varepsilon_t \varepsilon_0 T_0 dt + \int_{T_0}^T \frac{\varepsilon_t \varepsilon_0}{2\mu t} + \frac{\varepsilon_t \varepsilon_{t/2} \ln t}{2\mu} dt.$$

Recall that $\varepsilon_t = \min(1, \frac{1}{\sqrt{t}})$, and that $T_0 \geq 2$. Thus

$$\int_0^T \int_0^t \varepsilon_t \varepsilon_s e^{2\mu(s-t)} ds \leq \int_0^{T_0} \varepsilon_0 T_0 dt + \frac{\varepsilon_0}{2\mu} \int_{T_0}^T \frac{\varepsilon_t}{t} dt + \frac{\ln T}{2\mu} \int_2^T \varepsilon_t \varepsilon_{t/2} dt.$$

The first two integrals are converging when $T \rightarrow \infty$ and the last integral is $\mathcal{O}(\ln T)$. Plugging this into (23), we finally obtain the existence of a constant $c > 0$ such that

$$\frac{1}{T} \int_0^T \|\nabla \ell(\theta_t)\|^2 dt \leq \frac{c(\ln T)^2}{T^{1/2}}.$$

B.2. Langevin with discrete flow—proof of Theorem 4.7

We take

$$\gamma_k = \frac{1}{k^{1/3}} \min\left(\frac{1}{L_X}, \frac{1}{\sqrt{L_\Theta}}, \frac{1}{\mu}, \frac{\mu}{4L_X^2}\right) \quad \text{and} \quad \varepsilon_k = \frac{1}{k^{1/3}}. \quad (24)$$

Bounding the KL divergence of p_{k+1} from $\pi^*(\theta_{k+1})$. Recall that p_k is the law of X_k . We leverage similar ideas to Vempala & Wibisono (2019, Lemma 3) to bound the KL along one Langevin Monte Carlo iteration. The starting point is to notice that one Langevin Monte Carlo iteration can be equivalently written as a continuous-time process over a small time interval $[0, \gamma_k]$. More precisely, let

$$\rho_0 := p_k, \quad x_0 \sim \rho_0,$$

and x_t satisfying the SDE

$$dx_t = -\nabla_1 V(x_0, \theta_k) dt + \sqrt{2} dB_t.$$

Then, following the proof of Vempala & Wibisono (2019, Lemma 3), p_{k+1} has the same distribution as the output at time $\gamma := \gamma_k$ of the continuity equation

$$\frac{\partial \rho_t}{\partial t} [x] = \nabla \cdot (\rho_t [x] (\mathbb{E}_{\rho_{0|t}} [\nabla_1 V(x_k, \theta_k) | x_t = x] + \nabla \log \rho_t))$$

where $\rho_{0|t}$ is the conditional distribution of x_0 given x_t . Similarly, θ_{k+1} is equal to the output at time γ of

$$\vartheta_t := \theta_k - t \varepsilon_k \Gamma(\mu_k, \theta_k). \quad (25)$$

We have:

$$\frac{d \text{KL}(\rho_t || \pi^*(\vartheta_t))}{dt} = \int \log \left(\frac{\rho_t}{\pi^*(\vartheta_t)} \right) \frac{\partial \rho_t}{\partial t} + \int \frac{\rho_t}{\pi^*(\vartheta_t)} \frac{\partial \pi^*(\vartheta_t)}{\partial t} := a + b.$$

We first bound b similarly to the proof of Theorem 4.5, under Assumptions 4.2 and 4.3:

$$b = \varepsilon_k \int \langle \nabla_2 V(x, \vartheta_t) - \mathbb{E}_{X \sim \pi^*(\vartheta_t)}(\nabla_2 V(X, \vartheta_t)), \Gamma(\mu_k, \theta_k) \rangle p_t[x] dx \leq 2\varepsilon_k C^2.$$

Then we write a as

$$\begin{aligned} a &= \int \log\left(\frac{\rho_t[x]}{\pi^*(\vartheta_t)[x]}\right) \nabla \cdot (\rho_t[x] (\mathbb{E}_{\rho_{0t}}[\nabla_1 V(x_0, \theta_k)|x_t = x] + \nabla \log \rho_t[x])) dx \\ &= - \int \rho_t(x) \left\langle \nabla \log\left(\frac{\rho_t[x]}{\pi^*(\vartheta_t)[x]}\right), \mathbb{E}_{\rho_{0t}}[\nabla_1 V(x_0, \theta_k)|x_t = x] + \nabla \log \rho_t[x] \right\rangle dx \\ &= - \int \rho_t(x) \left\langle \nabla \log\left(\frac{\rho_t[x]}{\pi^*(\vartheta_t)[x]}\right), \mathbb{E}_{\rho_{0t}}[\nabla_1 V(x_0, \theta_k)|x_t = x] - \nabla_1 V(x, \theta_k) + \nabla_1 V(x, \theta_k) \right. \\ &\quad \left. - \nabla_1 V(x, \vartheta_t) + \nabla \log\left(\frac{\rho_t[x]}{\pi^*(\vartheta_t)[x]}\right) \right\rangle dx \\ &= - \int \rho_t \left\| \nabla \log\left(\frac{\rho_t}{\pi^*(\vartheta_t)}\right) \right\|^2 + \int \rho_t[x] \left\langle \nabla \log\left(\frac{\rho_t[x]}{\pi^*(\vartheta_t)[x]}\right), \nabla_1 V(x, \theta_k) - \mathbb{E}_{\rho_{0t}}[\nabla_1 V(x_0, \theta_k)|x_t = x] \right\rangle dx \\ &+ \int \rho_t[x] \left\langle \nabla \log\left(\frac{\rho_t[x]}{\pi^*(\vartheta_t)[x]}\right), \nabla_1 V(x, \vartheta_t) - \nabla_1 V(x, \theta_k) \right\rangle dx \\ &=: a_1 + a_2 + a_3. \end{aligned}$$

Denote the Fisher divergence by

$$\text{FD}(\rho_t \parallel \pi^*(\vartheta_t)) := \int \rho_t \left\| \nabla \log\left(\frac{\rho_t}{\pi^*(\vartheta_t)}\right) \right\|^2.$$

The first term a_1 is equal to $-\text{FD}(\rho_t \parallel \pi^*(\vartheta_t))$. To bound the second term a_2 , denote ρ_{0t} the joint distribution of (x_0, x_t) . Then

$$a_2 = \int \rho_{0t}[x_0, x_t] \langle \nabla \log\left(\frac{\rho_t[x_t]}{\pi^*(\vartheta_t)[x_t]}\right), \nabla_1 V(x_t, \theta_k) - \nabla_1 V(x_0, \theta_k) \rangle dx_0 dx_t$$

Using $\langle a, b \rangle \leq \|a\|^2 + \frac{1}{4}\|b\|^2$ and recalling that $x \mapsto \nabla_1 V(x, \theta)$ is L_X -Lipschitz for all $\theta \in \mathbb{R}^p$ by Assumption 4.6,

$$\begin{aligned} a_2 &\leq \mathbb{E}_{(x_0, x_t) \sim \rho_{0t}} \|\nabla_1 V(x_t, \theta_k) - \nabla_1 V(x_0, \theta_k)\|^2 + \frac{1}{4} \mathbb{E}_{(x_0, x_t) \sim \rho_{0t}} \left\| \nabla \log\left(\frac{\rho_t[x_t]}{\pi^*(\vartheta_t)[x_t]}\right) \right\|^2 \\ &\leq L_X^2 \mathbb{E}_{(x_0, x_t) \sim \rho_{0t}} \|x_t - x_0\|^2 + \frac{1}{4} \text{FD}(\rho_t \parallel \pi^*(\vartheta_t)). \end{aligned}$$

Proceeding similarly for a_3 , we obtain

$$a_3 \leq \mathbb{E}_{x \sim \rho_t} \|\nabla_1 V(x, \vartheta_t) - \nabla_1 V(x, \theta_k)\|^2 + \frac{1}{4} \text{FD}(\rho_t \parallel \pi^*(\vartheta_t)).$$

Since $\theta \mapsto \nabla_1 V(x, \theta)$ is L_Θ -Lipschitz for all $x \in \mathbb{R}^d$ by Assumption 4.6, we get

$$a_3 \leq L_\Theta \|\vartheta_t - \theta_k\|^2 + \frac{1}{4} \text{FD}(\rho_t \parallel \pi^*(\vartheta_t)).$$

Moreover, by (25) and under Assumption 4.3, we have $\|\vartheta_t - \theta_k\|^2 = t^2 \varepsilon_k^2 \|\Gamma(\mu_k, \theta_k)\|^2 \leq t^2 \varepsilon_k^2 C^2$, which yields

$$a_3 \leq L_\Theta t^2 \varepsilon_k^2 C^2 + \frac{1}{4} \text{FD}(\rho_t \parallel \pi^*(\vartheta_t)).$$

Putting everything together,

$$\begin{aligned} \frac{d \text{KL}(\rho_t \parallel \pi^*(\vartheta_t))}{dt} &= a + b \leq -\frac{1}{2} \text{FD}(\rho_t \parallel \pi^*(\vartheta_t)) + L_X^2 \mathbb{E}_{(x_0, x_t) \sim \rho_{0t}} \|x_t - x_0\|^2 + L_\Theta t^2 \varepsilon_k^2 C^2 + 2\varepsilon_k C^2 \\ &\leq -\mu \text{KL}(\rho_t \parallel \pi^*(\vartheta_t)) + L_X^2 \mathbb{E}_{(x_0, x_t) \sim \rho_{0t}} \|x_t - x_0\|^2 + L_\Theta t^2 \varepsilon_k^2 C^2 + 2\varepsilon_k C^2 \end{aligned}$$

where the last inequality uses Assumption 4.1 and where the two last terms in the r.h.s. can be seen as additional bias terms compared to the analysis of Vempala & Wibisono (2019, Lemma 3). Let us now bound $\mathbb{E}_{(x_0, x_t) \sim \rho_{0t}} \|x_t - x_0\|^2$. Recall that $x_t \stackrel{d}{=} x_0 - t\nabla_1 V(x_0, \theta_k) + \sqrt{2t}z_0$, where $z_0 \sim \mathcal{N}(0, I)$ is independent of x_0 . Then

$$\begin{aligned} \mathbb{E}_{(x_0, x_t) \sim \rho_{0t}} \|x_t - x_0\|^2 &= \mathbb{E}_{(x_0, x_t) \sim \rho_{0t}} \left\| -t\nabla_1 V(x_0, \theta_k) + \sqrt{2t}z_0 \right\|^2 \\ &= t^2 \mathbb{E}_{x_0 \sim \rho_0} \|\nabla_1 V(x_0, \theta_k)\|^2 + 2td. \end{aligned}$$

Finally, since $x \mapsto \nabla_1 V(x, \theta)$ is L_X -Lipschitz for all $x \in \mathbb{R}^d$ by Assumption 4.6, and under Assumption 4.1, we get by Vempala & Wibisono (2019, Lemma 12) that

$$\mathbb{E}_{x_0 \sim \rho_0} \|\nabla_1 V(x_0, \theta_k)\|^2 \leq \frac{4L_X^2}{\mu} \text{KL}(\rho_0 \parallel \pi^*(\theta_k)) + 2dL_X.$$

All in all,

$$\frac{d \text{KL}(\rho_t \parallel \pi^*(\vartheta_t))}{dt} \leq -\mu \text{KL}(\rho_t \parallel \pi^*(\vartheta_t)) + \frac{4L_X^4 t^2}{\mu} \text{KL}(\rho_0 \parallel \pi^*(\theta_k)) + 2dL_X^3 t^2 + 2L_X^2 t d + L_\Theta t^2 \varepsilon_k^2 C^2 + 2\varepsilon_k C^2.$$

Recall that we want to integrate t between 0 and γ . For $t \leq \gamma$, we have

$$\begin{aligned} \frac{d \text{KL}(\rho_t \parallel \pi^*(\vartheta_t))}{dt} &\leq -\mu \text{KL}(\rho_t \parallel \pi^*(\vartheta_t)) + \frac{4L_X^4 \gamma^2}{\mu} \text{KL}(\rho_0 \parallel \pi^*(\theta_k)) + 2dL_X^3 \gamma^2 + 2L_X^2 \gamma d + L_\Theta \gamma^2 \varepsilon_k^2 C^2 + 2\varepsilon_k C^2 \\ &\leq -\mu \text{KL}(\rho_t \parallel \pi^*(\vartheta_t)) + \frac{4L_X^4 \gamma^2}{\mu} \text{KL}(\rho_0 \parallel \pi^*(\theta_k)) + 4L_X^2 \gamma d + 3\varepsilon_k C^2 \end{aligned}$$

since $L_X \gamma \leq 1$, $L_\Theta \gamma^2 \leq 1$ and $\varepsilon_k \leq 1$ by (24). Denote by C_1 the second term and C_2 the sum of the last two terms. Then, by Grönwall's inequality (Pachpatte & Ames, 1997),

$$\text{KL}(\rho_t \parallel \pi^*(\vartheta_t)) \leq \frac{(C_1 + C_2)e^{-\mu t}(e^{\mu t} - 1)}{\mu} + \text{KL}(\rho_0 \parallel \pi^*(\theta_k))e^{-\mu t}.$$

Since $\mu t \leq \mu \gamma \leq 1$ by (24), we have $e^{\mu t} \leq 1 + 2\mu\gamma$, and

$$\begin{aligned} \text{KL}(\rho_t \parallel \pi^*(\vartheta_t)) &\leq 2(C_1 + C_2)\gamma e^{-\mu t} + \text{KL}(\rho_0 \parallel \pi^*(\theta_k))e^{-\mu t} \\ &= 2C_2\gamma e^{-\mu t} + \left(1 + \frac{8L_X^4 \gamma^3}{\mu}\right) \text{KL}(\rho_0 \parallel \pi^*(\theta_k))e^{-\mu t}. \end{aligned}$$

Since $\gamma \leq \frac{\mu}{4L_X^2}$ by (24), we have $\frac{8L_X^4 \gamma^3}{\mu} \leq \frac{\mu\gamma}{2}$, and

$$\text{KL}(\rho_t \parallel \pi^*(\vartheta_t)) \leq 2C_2\gamma e^{-\mu t} + \left(1 + \frac{\mu\gamma}{2}\right) \text{KL}(\rho_0 \parallel \pi^*(\theta_k))e^{-\mu t}.$$

We therefore obtain, by evaluating at $t = \gamma$ and renaming $p_{k+1} = \rho_\gamma$, $\pi^*(\theta_{k+1}) = \pi^*(\vartheta_\gamma)$, $p_k = \rho_0$, and $\gamma_k = \gamma$,

$$\text{KL}(p_{k+1} \parallel \pi^*(\theta_{k+1})) \leq 2C_2\gamma_k e^{-\mu\gamma_k} + \left(1 + \frac{\mu\gamma_k}{2}\right) \text{KL}(p_k \parallel \pi^*(\theta_k))e^{-\mu\gamma_k}.$$

Bounding the KL over the whole dynamics. Let $C_3 := (1 + \frac{\mu\gamma_k}{2})e^{-\mu\gamma_k}$. We have $C_3 < 1$, and by summing and telescoping,

$$\text{KL}(p_k \parallel \pi^*(\theta_k)) \leq \text{KL}(p_0 \parallel \pi^*(\theta_0))C_3^k + \frac{2C_2C_3\gamma_k e^{-\mu\gamma_k}}{1 - C_3}.$$

We have

$$\frac{C_3 e^{-\mu\gamma_k}}{1 - C_3} = \frac{C_3}{e^{\mu\gamma_k} - (1 + \frac{\mu\gamma_k}{2})} \leq \frac{2}{\mu\gamma_k},$$

by using $e^x \geq 1 + x$ and $C_3 \leq 1$. Thus

$$\text{KL}(p_k \parallel \pi^*(\theta_k)) \leq \text{KL}(p_0 \parallel \pi^*(\theta_0))C_3^k + \frac{4C_2}{\mu}.$$

Replacing C_2 by its value,

$$\text{KL}(p_k \parallel \pi^*(\theta_k)) \leq \text{KL}(p_0 \parallel \pi^*(\theta_0))C_3^k + \frac{16L_X^2 d\gamma_k}{\mu} + \frac{12C^2 \varepsilon_k}{\mu}.$$

Since $e^x \geq 1 + x$, $C_3 \leq e^{-\mu\gamma_k/2}$, and

$$\text{KL}(p_k \parallel \pi^*(\theta_k)) \leq \text{KL}(p_0 \parallel \pi^*(\theta_0))e^{-\frac{\mu\gamma_k k}{2}} + \frac{16L_X^2 d\gamma_k}{\mu} + \frac{12C^2 \varepsilon_k}{\mu}. \quad (26)$$

We obtain three terms in our bound that have different origins. The first term corresponds to an exponential decay of the KL divergence at initialization. The second term is linked to the discretization error, and is proportional to γ_k . The third term is due to the fact that $\pi^*(\theta_k)$ is moving due to the outer problem updates (14). It is proportional to the ratio of learning rates ε_k .

Evolution of the loss. By Assumption 4.6, the loss ℓ is L -smooth, and recall that $\theta_{k+1} = \theta_k - \gamma_k \varepsilon_k \Gamma(p_k, \theta_k)$. We have

$$\begin{aligned} \ell(\theta_{k+1}) &= \ell(\theta_k - \gamma_k \varepsilon_k \Gamma(p_k, \theta_k)) \\ &\leq \ell(\theta_k) - \gamma_k \varepsilon_k \langle \nabla \ell(\theta_k), \Gamma(p_k, \theta_k) \rangle + \frac{L\gamma_k^2 \varepsilon_k^2}{2} \|\Gamma(p_k, \theta_k)\|^2 \\ &\leq \ell(\theta_k) - \gamma_k \varepsilon_k \langle \nabla \ell(\theta_k), \Gamma(p_k, \theta_k) \rangle + \frac{LC^2 \gamma_k^2 \varepsilon_k^2}{2} \end{aligned}$$

by Assumption 4.3. Furthermore,

$$\Gamma(\mu_k, \theta_k) = \Gamma(\pi^*(\theta_k), \theta_k) + \Gamma(p_k, \theta_k) - \Gamma(\pi^*(\theta_k), \theta_k) = \nabla \ell(\theta_k) + \Gamma(p_k, \theta_k) - \Gamma(\pi^*(\theta_k), \theta_k).$$

Thus

$$\begin{aligned} \ell(\theta_{k+1}) &\leq \ell(\theta_k) - \gamma_k \varepsilon_k \|\nabla \ell(\theta_k)\|^2 + \gamma_k \varepsilon_k \|\nabla \ell(\theta_k)\| \|\Gamma(p_k, \theta_k) - \Gamma(\pi^*(\theta_k), \theta_k)\| + \frac{LC^2 \gamma_k^2 \varepsilon_k^2}{2} \\ &\leq \ell(\theta_k) - \gamma_k \varepsilon_k \|\nabla \ell(\theta_k)\|^2 + \gamma_k \varepsilon_k \|\nabla \ell(\theta_k)\| \sqrt{\text{KL}(p_k \parallel \pi^*(\theta_k))} + \frac{LC^2 \gamma_k^2 \varepsilon_k^2}{2} \end{aligned}$$

by Assumption 4.3. Using $ab \leq \frac{1}{2}(a^2 + b^2)$, we obtain

$$\ell(\theta_{k+1}) \leq \ell(\theta_k) - \frac{\gamma_k \varepsilon_k}{2} \|\nabla \ell(\theta_k)\|^2 + \frac{\gamma_k \varepsilon_k}{2} \text{KL}(p_k \parallel \pi^*(\theta_k)) + \frac{LC^2 \gamma_k^2 \varepsilon_k^2}{2}.$$

Conclusion. Summing and telescoping,

$$\ell(\theta_{K+1}) - \ell(\theta_1) \leq -\frac{1}{2} \sum_{k=1}^K \gamma_k \varepsilon_k \|\nabla \ell(\theta_k)\|^2 + \frac{1}{2} \sum_{k=1}^K \gamma_k \varepsilon_k \text{KL}(p_k \parallel \pi^*(\theta_k)) + \frac{LC^2}{2} \sum_{k=1}^K \gamma_k^2 \varepsilon_k^2.$$

Lower bounding γ_k by γ_K and ε_k by ε_K in the first sum, then reorganizing terms, we obtain

$$\frac{1}{K} \sum_{k=1}^K \|\nabla \ell(\theta_k)\|^2 \leq \frac{2(\ell(\theta_1) - \inf \ell)}{K \gamma_K \varepsilon_K} + \frac{1}{K \gamma_K \varepsilon_K} \sum_{k=1}^K \gamma_k \varepsilon_k \text{KL}(p_k \parallel \pi^*(\theta_k)) + \frac{LC^2}{K \gamma_K \varepsilon_K} \sum_{k=1}^K \gamma_k^2 \varepsilon_k^2.$$

Bounding the KL divergence by (26), we get

$$\begin{aligned} \frac{1}{K} \sum_{k=1}^K \|\nabla \ell(\theta_k)\|^2 &\leq \frac{2(\ell(\theta_1) - \inf \ell)}{K \gamma_K \varepsilon_K} + \frac{1}{K \gamma_K \varepsilon_K} \sum_{k=1}^K \text{KL}(p_0 \parallel \pi^*(\theta_0)) \gamma_k \varepsilon_k e^{-\frac{\mu\gamma_k k}{2}} + \frac{1}{K \gamma_K \varepsilon_K} \sum_{k=1}^K \frac{16L_X^2 d\gamma_k^2 \varepsilon_k}{\mu} \\ &\quad + \frac{1}{K \gamma_K \varepsilon_K} \sum_{k=1}^K \frac{12C^2 \gamma_k \varepsilon_k^2}{\mu} + \frac{LC^2 \gamma}{K \gamma_K \varepsilon_K} \sum_{k=1}^K \gamma_k^2 \varepsilon_k^2. \end{aligned}$$

By definition (24) of γ_k and ε_k , we see that the first and last sums are converging, and the middle sums are $\mathcal{O}(\ln K)$. Therefore, we obtain

$$\frac{1}{K} \sum_{k=1}^K \|\nabla \ell(\theta_k)\|^2 \leq \frac{c \ln K}{K^{1/3}}$$

for some $c > 0$ depending only on the constants of the problem.

B.3. Denoising diffusion

Our goal is first to find a continuous-time equivalent of Algorithm 3. To this aim, we first introduce a slightly different version of the algorithm where the queue of M versions of p_k is not present at initialization, but constructed during the first M steps of the algorithm. As a consequence, θ changes for the first time after M steps of the algorithm, when the queue is completed and the M -th element of the queue has been processed through all the sampling steps.

Algorithm 7 Implicit Diff. optimization, finite time (no warm start)

input $\theta_0 \in \mathbb{R}^p, p_0 \in \mathcal{P}$
 $p_0^{(0)} \leftarrow p_0$
for $k \in \{0, \dots, K-1\}$ (joint single loop) **do**
 $p_{k+1}^{(0)} \leftarrow p_0$
parallel $p_{k+1}^{(m+1)} \leftarrow \Sigma_m(p_k^{(m)}, \theta_k)$ for $m \in [\min(k, M-1)]$
if $k \geq M$ **then**
 $\theta_{k+1} \leftarrow \theta_k - \eta_k \Gamma(p_k^{(M)}, \theta_k)$ (or another optimizer)
output θ_K

In order to obtain the continuous-time equivalent of Algorithm 7, it is convenient to change indices defining $p_k^{(m)}$. Note that in the update of $p_k^{(m)}$ in the algorithm, the quantity $m - k$ is constant. Therefore, denoting $j = m - k$, the algorithm above is exactly equivalent to

$$\begin{aligned} p_j^{(0)} &= p_0 \\ p_j^{(m+1)} &= \Sigma_m(p_j^{(m)}, \theta_{j+m}), \quad m \in [M-1] \\ \theta_{k+1} &= \theta_k \quad \text{if } k < M \\ \theta_{k+1} &= \theta_k - \eta_k \Gamma(p_{k-M}^{(M)}, \theta_k) \quad \text{else.} \end{aligned}$$

It is then possible to translate this algorithm in a continuous setting in the case of denoising diffusions. We obtain

$$\begin{aligned} Y_t^0 &\sim \mathcal{N}(0, 1) \\ dY_t^\tau &= \{Y_t^\tau + 2s_{\theta_{t+\tau}}(Y_t^\tau, T - \tau)\}d\tau + \sqrt{2}dB_\tau \\ d\theta_t &= 0 \quad \text{for } t < T \\ d\theta_t &= -\eta_k \Gamma(Y_{t-T}^T, \theta_t)dt \quad \text{for } t \geq T, \end{aligned} \tag{27}$$

Let us choose the score function s_θ as in Section 4.3. The backward equation (7) then writes

$$dY_t = (Y_t + 2s_\theta(Y_t, T - t))dt + \sqrt{2}dB_t = -(Y_t - 2\theta e^{-(T-t)})dt + \sqrt{2}dB_t. \tag{28}$$

We now turn our attention to the computation of Γ . Recall that Γ should satisfy $\Gamma(\pi^*(\theta), \theta) = \nabla \ell(\theta)$, where $\pi^*(\theta)$ is the distribution of Y_T and $\ell(\theta) = \mathbb{E}_{Y \sim \pi^*(\theta)}(L(Y))$ for some loss function $L : \mathbb{R} \rightarrow \mathbb{R}$. To this aim, for a given realization of the SDE (28), let us compute the derivative of $L(Y_T)$ with respect to θ using the adjoint method (16). We have $\nabla_2 \mu(T - t, Y_{T-t}, \theta) = -1$, hence $\frac{dA_t}{dt} = -1$, and $A_t = L'(Y_T)e^{-t}$. Furthermore, $\nabla_3 \mu(T - t, Y_{T-t}, \theta) = 2e^{-t}$. Thus

$$\frac{dL(Y_T)}{d\theta} = \int_0^T A_t \nabla_3 \mu(T - t, Y_{T-t}, \theta) dt = \int_0^T 2L'(Y_T)e^{-2t} dt = L'(Y_T)(1 - e^{-2T}).$$

As a consequence,

$$\nabla \ell(\theta) = \mathbb{E}_{Y \sim q_T^*(\theta)} \left(\frac{dL(Y)}{d\theta} \right) = \mathbb{E}_{Y \sim q_T^*(\theta)} (L'(Y)(1 - e^{-2T})).$$

This prompts us to define

$$\Gamma(p, \theta) = \mathbb{E}_{X \sim p}(L'(X)(1 - e^{-2T})) = \mathbb{E}_{X \sim p}((X - \theta_{\text{target}})(1 - e^{-2T})) = (\mathbb{E}_{X \sim p} X - \theta_{\text{target}})(1 - e^{-2T})$$

for L defined by $L(x) = (x - \theta_{\text{target}})^2$ as in Section 4.3. Note that, in this case, Γ depends only on p and not on θ .

Replacing s_θ and Γ by their values in (27), we obtain the coupled differential equations in Y and θ

$$\begin{aligned} Y_t^0 &\sim \mathcal{N}(0, 1) \\ dY_t^\tau &= \{-Y_t^\tau + 2\theta_{t+\tau}e^{-(T-\tau)}\}d\tau + \sqrt{2}dB_\tau \\ d\theta_t &= 0 \quad \text{for } t < T \\ d\theta_t &= -\eta(\mathbb{E}Y_{t-T}^T - \theta_{\text{target}})(1 - e^{-2T})dt \quad \text{for } t \geq T, \end{aligned} \tag{29}$$

We can now formalize Proposition 4.8, with the following statement.

Proposition B.3. *Consider the dynamics (29). Then*

$$\|\theta_{2T} - \theta_{\text{target}}\| = \mathcal{O}(e^{-T}), \quad \text{and} \quad \pi^*(\theta_{2T}) = \mathcal{N}(\mu, 1) \text{ with } \mu = \theta_{\text{target}} + \mathcal{O}(e^{-T}).$$

Proof. Let us first compute the expectation of Y_t^τ . To this aim, denote $Z_t^\tau = e^\tau Y_t^\tau$. Then we have

$$dZ_t^\tau = e^\tau(dY_t^\tau + Y_t^\tau dt) = 2\theta_{t+\tau}e^{2\tau-T}d\tau + \sqrt{2}dB_\tau.$$

Since $\mathbb{E}(Z_t^0) = \mathbb{E}(Y_t^0) = 0$, we obtain that $\mathbb{E}(Z_t^T) = 2 \int_0^T \theta_{t+\tau}e^{2(\tau-T)}d\tau$, and

$$\mathbb{E}(Y_t^T) = e^{-T}\mathbb{E}(Z_t^T) = 2 \int_0^T \theta_{t+\tau}e^{2(\tau-T)}d\tau.$$

Therefore, we obtain the following evolution equation for θ when $t \geq T$:

$$\dot{\theta}_t = -\eta \left(2 \int_0^T \theta_{t-T+\tau}e^{2(\tau-T)}d\tau - \theta_{\text{target}} \right) (1 - e^{-2T}).$$

By the change of variable $\tau \leftarrow T - \tau$ in the integral, we have, for $t \geq T$,

$$\dot{\theta}_t = -\eta \left(2 \int_0^T \theta_{t-\tau}e^{-2\tau}d\tau - \theta_{\text{target}} \right) (1 - e^{-2T}).$$

Let us introduce the auxiliary variable $\psi_t = \int_0^T \theta_{t-\tau}e^{-2\tau}d\tau$. We have $\dot{\theta}_t = -\eta(2\psi_t - \theta_{\text{target}})$, and

$$\dot{\psi}_t = \int_0^T \dot{\theta}_{t-\tau}e^{-2\tau}d\tau = -[\theta_{t-\tau}e^{-2\tau}]_0^T - 2 \int_0^T \theta_{t-\tau}e^{-2\tau}d\tau = \theta_t - \theta_{t-T}e^{-2T} - 2\psi_t.$$

Recall that θ_t is constant equal to θ_0 for $t \in [0, T]$. Therefore, for $t \in [T, 2T]$, $\xi := (\theta, \psi)$ satisfies the first order linear ODE with constant coefficients

$$\dot{\xi} = A\xi + b, \quad A = \begin{pmatrix} 0 & -2\eta \\ 1 & -2 \end{pmatrix}, \quad b = \begin{pmatrix} \eta\theta_{\text{target}}(1 - e^{-2T}) \\ -\theta_0e^{-2T} \end{pmatrix}.$$

For $\eta > 0$, A is invertible, and

$$A^{-1} = \frac{1}{2\eta} \begin{pmatrix} -2 & 2\eta \\ -1 & 0 \end{pmatrix}.$$

Hence the linear ODE has solution, for $t \in [T, 2T]$,

$$\xi_t = -(I - e^{(t-T)A})A^{-1}b + e^{(t-T)A}\xi_T = -A^{-1}b + e^{(t-T)A}(A^{-1}b + \xi_T).$$

Thus

$$\xi_{2T} = -A^{-1}b + e^{TA}(A^{-1}b + \xi_T) = -A^{-1}b + e^{TA} \left(A^{-1}b + \begin{pmatrix} \theta_0 \\ \frac{\theta_0(1-e^{-2T})}{2} \end{pmatrix} \right).$$

A straightforward computation shows that

$$[A^{-1}b]_0 = -\theta_{\text{target}}(1 - e^{-2T}) + \theta_0e^{-2T},$$

and that A has eigenvalues with negative real part. Putting everything together, we obtain

$$\theta_{2T} = [\xi_{2T}]_0 = \theta_{\text{target}} + \mathcal{O}(e^{-T}).$$

Finally, recall that we have $\pi^*(\theta) = \mathcal{N}(\theta(1 - e^{-2T}), 1)$. Thus $\pi^*(\theta_{2T}) = \mathcal{N}(\mu_{2T}, 1)$ with $\mu_{2T} = \theta_{\text{target}} + \mathcal{O}(e^{-T})$. \square

C. Experimental details

We provide here details about our experiments in Section 5.

C.1. Langevin processes

We consider a parameterized family of potentials for $x \in \mathbb{R}^2$ and $\theta \in \mathbb{R}^6$ defined by

$$V(x, \theta) = -\log \left(\sum_{i=1}^6 \sigma(\theta)_i \exp(-\|x - \mu_i\|^2) \right),$$

where the $\mu_i \in \mathbb{R}^2$ are the six vertices of a regular hexagon and σ is the softmax function mapping \mathbb{R}^6 to the unit simplex. In this setting, for any $\theta \in \mathbb{R}^6$,

$$\pi^*(\theta) = \frac{1}{Z} \sum_{i=1}^6 \sigma(\theta)_i \exp(-\|x - \mu_i\|^2),$$

where Z is an absolute renormalization constant that is independent of θ . This simplifies drawing contour lines, but we do not use this prior knowledge in our algorithms, and only use calls to functions $\nabla_1 V(\cdot, \theta)$ and $\nabla_2 V(\cdot, \theta)$ for various $\theta \in \mathbb{R}^6$.

We run four sampling algorithms, all initialized with $p_0 = \mathcal{N}(0, I_2)$. For all of them we generate a batch of variables $X^{(i)}$ of size 1,000, all initialized independently with $X_0^{(i)} \sim \mathcal{N}(0, I_2)$. The sampling and optimization steps are realized in parallel over the batch. The samples are represented after $T = 5,000$ steps of each algorithm in Figure 4, and used to compute the values of reward and likelihood reported in Figure 5. We also display in Figure 7 the dynamics of the probabilities throughout these algorithms.

We provide here additional details and motivation about these algorithms, denoted by the colored markers that represent them in these figures.

- Langevin θ_0 (■): This is the discrete-time process (a Langevin Monte Carlo process) approximating a Langevin diffusion with potential $V(\cdot, \theta_0)$ for fixed $\theta_0 := (1, 0, 1, 0, 1, 0)$. There is no reward here, the time-continuous Langevin process converges to $\pi^*(\theta_0)$, that has some symmetries. It can be thought of as a pretrained model, and the Langevin sampling algorithm as an inference-time generative algorithm.
- **Implicit Diffusion** (★): We run the infinite-time horizon version of our method (Algorithm 2), aiming to minimize

$$\ell(\theta) := \mathcal{F}(\pi^*(\theta)) \quad \text{for} \quad \mathcal{F}(p) = -\mathbb{E}_{X \sim p}[R(X)] \quad \text{with} \quad R(x) = \mathbf{1}(x_1 > 0) \exp(-\|x - \mu\|^2),$$

where $\mu = (1, 0.95)$. This algorithm yields both a sample \hat{p}_T and parameters θ_{opt} after T steps, and can be thought of as jointly sampling and reward finetuning.

- Langevin $\theta_0 + R$ (▼): This is a discrete-time process approximating a Langevin diffusion with reward-guided potential $V(\cdot, \theta_0) - \lambda R_{\text{smooth}}$, where R_{smooth} is a smoothed version of R (replacing the indicator by a sigmoid). Using this approach is different from finetuning: it proposes to modify the sampling algorithm, and does not yield new parameters θ . This is akin to guidance of generative models (Dhariwal & Nichol, 2021). Note that this approach requires a differentiable reward R_{smooth} , contrarily to our approach that handles non-differentiable rewards.
- Langevin θ_{opt} - post **Implicit Diffusion** (●): This is a discrete-time process approximating a Langevin diffusion with potential $V(\cdot, \theta_{\text{opt}})$, where θ_{opt} is the outcome of reward training by our algorithm. This can be thought of as doing inference with the new model parameters, post reward training with Implicit Diffusion.

As mentioned in Section 5.1, this illustrative setting allows to illustrate the advantage of our method, which efficiently allows to optimize a function over a constrained set of distribution, without overfitting outside this class. We display in Figure 7 snapshots throughout some selected steps of these four algorithms (in the same order and with the same colors as indicated above). We observe that the dynamics of Implicit Diffusion are slower than those of Langevin processes (sampling), which can be observed also in the metrics reported in Figure 5. The reward and log-likelihood change slowly, plateauing several times: when θ_k in this algorithm is initially close to θ_0 , the distribution gets closer to $\pi^*(\theta_0)$ (steps 0-100). It then evolves towards another distribution (steps 1000-2500), after θ has been affected by accurate gradient updates, before converging to

$\pi^*(\theta_{\text{opt}})$. These two-timescale dynamics is by design: the dynamics on the sampling dynamics are much faster, aiming to quickly lead to an accurate evaluation of gradients with respect to θ_k . This corresponds to our theoretical setting where $\varepsilon_k \ll 1$.

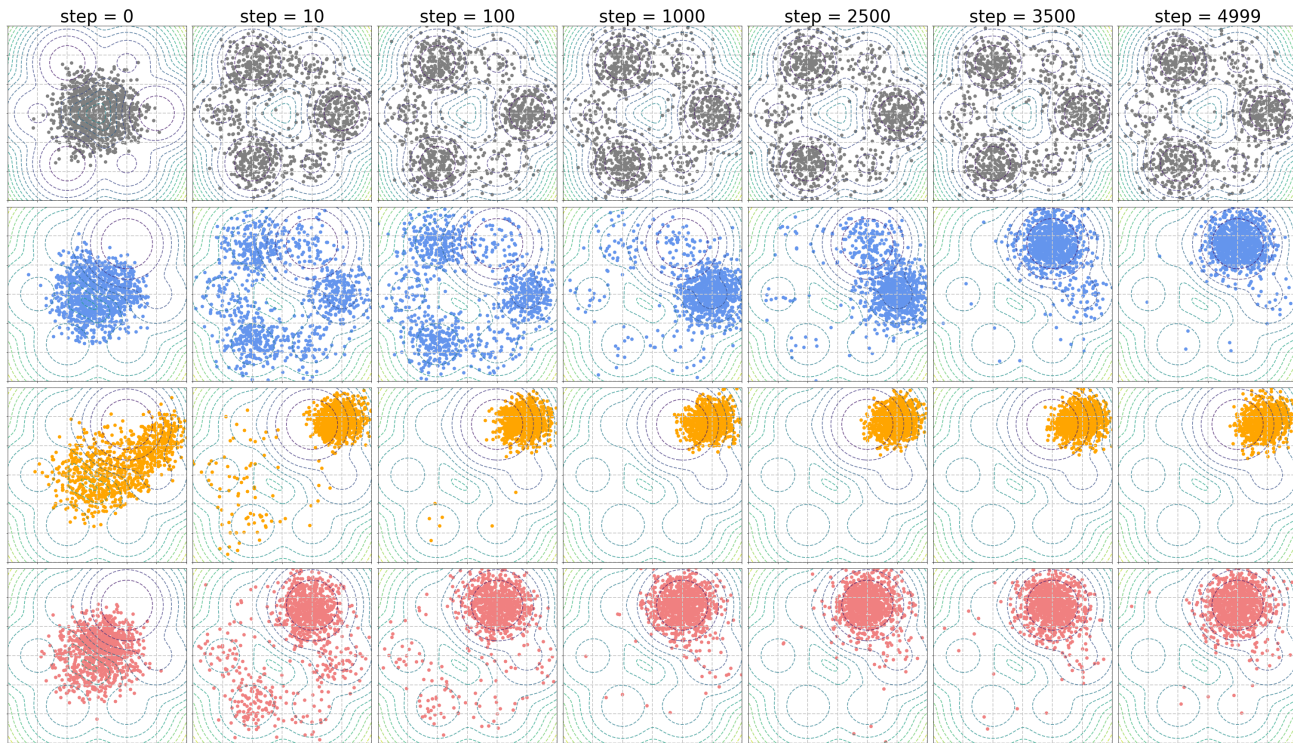


Figure 7. Dynamics of samples for four sampling algorithms at different time steps. **First:** Langevin θ_0 (●) with $\pi^*(\theta_0)$ contour lines. **Second:** Implicit Diffusion (●) with $\pi^*(\theta_{\text{opt}})$ contour lines. **Third:** Langevin θ_0 + smoothed Reward (●). **Fourth:** Langevin θ_{opt} (●).

C.2. Denoising diffusion models

We start by giving additional experimental configurations that are common between both datasets before explaining details specific to each one.

Common details. The KL term in the reward is computed using Girsanov’s theorem as explained in Appendix A.3. We use the Adam optimizer (Kingma & Ba, 2015), with various values for the learning rate (see e.g. Figure 6). The code was implemented in JAX (Bradbury et al., 2018).

MNIST. We use an Ornstein-Uhlenbeck noise schedule, meaning that the forward diffusion is $dX_t = -X_t dt + \sqrt{2} dB_t$ (as presented in Section 2.2). Further hyperparameters for pretraining and reward training are given respectively in Tables 1 and 2.

Name	Value
Noise schedule	Ornstein-Uhlenbeck
Optimizer	Adam with standard hyperparameters
EMA decay	0.995
Learning rate	10^{-3}
Batch size	32

Table 1. Hyperparameters for pretraining of denoising diffusion models on MNIST.

Implicit Diffusion

Name	Value
Number of sampling steps	256
Sampler	Euler
Noise schedule	Ornstein-Uhlenbeck
Optimizer	Adam with standard hyperparameters

Table 2. Hyperparameters for reward training of denoising diffusion models pretrained on MNIST.

CIFAR-10. Hyperparameters for pretraining and reward training are given respectively in Tables 3 and 4.

Name	Value
Number of sampling steps	1,024
Sampler	DDPM
Noise schedule	Cosine (Nichol & Dhariwal, 2021)
Optimizer	Adam with $\beta_1 = 0.9, \beta_2 = 0.99, \varepsilon = 10^{-12}$
EMA decay	0.9999
Learning rate	$2 \cdot 10^{-4}$
Batch size	2048
Number of samples for FID evaluation	50k

Table 3. Hyperparameters for pretraining of denoising diffusion models on CIFAR-10.

Name	Value
Number of sampling steps	1,024
Sampler	Euler
Noise schedule	Cosine (Nichol & Dhariwal, 2021)
Optimizer	Adam with standard hyperparameters

Table 4. Hyperparameters for reward training of denoising diffusion models pretrained on CIFAR-10.

Additional figures for MNIST. We showcase the results of our experiments, in Figures 10 and 11, by reporting metrics on the rewards and KL divergence with respect to the original distribution. Metrics are reported for various values of λ , both positive and negative. As in Figure 6 for CIFAR-10, we observe the competition between the reward and the divergence with respect to the distribution after pretraining. We also display in Figures 8 and 9 some selected examples of samples generated by our denoising diffusion model with parameters θ_k , at several steps k of our algorithm. Note that the random number generator system of JAX allows us, for illustration purposes, to sample for different parameters from the same seed. We take advantage of this feature to visualize the evolution of a given realization of the stochastic denoising process depending on θ .

Recall that we consider

$$\mathcal{F}(p) := -\lambda \mathbb{E}_{x \sim p}[R(x)] + \beta \text{KL}(p || \pi^*(\theta_0)),$$

where $R(x)$ is the average value of all the pixels in x . The figures present samples for negative and positive λ , rewarding respectively darker and brighter images. We emphasize that these samples are realized at different steps of our algorithm for evaluation purposes. To generate the samples, at various steps of the optimization procedure, we run the full denoising process for the current value of the parameters. In particular, these samples are different from the ones used to perform the joint sampling and parameter updates in **Implicit Diffusion**.

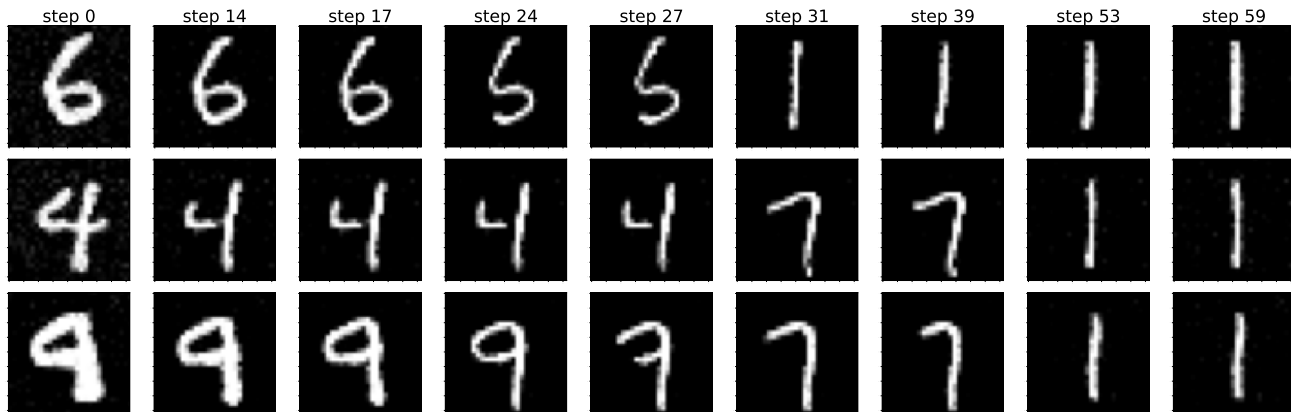


Figure 8. Reward training for a model pretrained on MNIST. Reward for **darker** images ($\lambda < 0, \beta > 0$). Selected examples are shown coming from a single experiment with $\lambda/\beta = -30$. All digits are re-sampled at the same selected steps of the Implicit Diffusion algorithm, as explained in Appendix C.2.

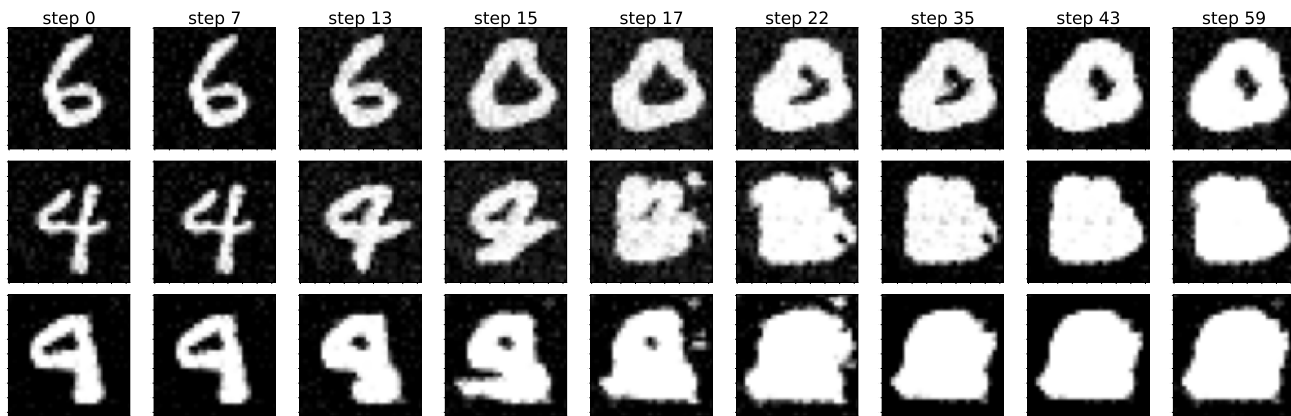


Figure 9. Reward training for a model pretrained on MNIST. Reward for **brighter** images ($\lambda > 0, \beta > 0$). Selected examples are shown coming from a single experiment with $\lambda/\beta = 30$. All digits are re-sampled at the same selected steps of the Implicit Diffusion algorithm, as explained in Appendix C.2.

We have purposefully chosen, for illustration purposes, samples for experiments with the highest magnitude of λ/β , i.e. those who favor reward optimization over proximity to the original distribution. As noted in Section 5, we observe qualitatively that reward training, while shifting some aspects of the distribution (here the average brightness), and necessarily diverging from the original pretrained model, manages to do so while retaining some global important characteristics of the dataset—even though the pretraining dataset is never observed during reward training. Since we chose to display samples from experiments with the most extreme incentives towards the reward, we observe that the similarity with the pretraining dataset can be forced to break down after a certain number of reward training steps. We also observe some mode collapse; we comment further on this point below.

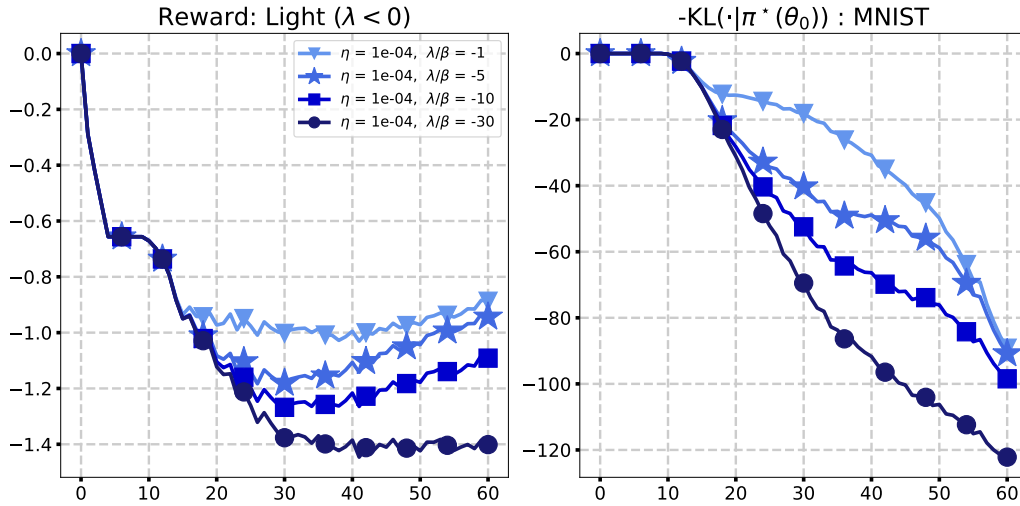


Figure 10. Score function reward training with **Implicit Diffusion** pretrained on MNIST for various $\lambda < 0$ (darker). **Left:** Reward, average brightness of image. **Right:** Divergence w.r.t. the original pretrained distribution.

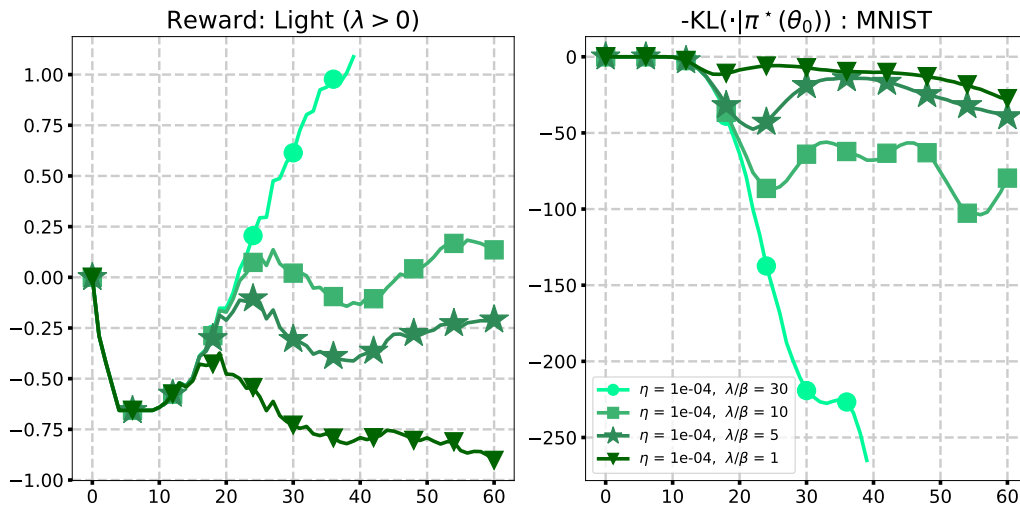


Figure 11. Score function reward training with **Implicit Diffusion** pretrained on MNIST for various $\lambda > 0$ (brighter). **Left:** Reward, average brightness of image. **Right:** Divergence w.r.t. the original pretrained distribution.

Additional figures for CIFAR-10. We recall that we consider, for a model with weights θ_0 pretrained on CIFAR-10, the objective function

$$\mathcal{F}(p) := -\lambda \mathbb{E}_{x \sim p}[R(x)] + \beta \text{KL}(p || \pi^*(\theta_0)),$$

where $R(x)$ is the average over the red channel, minus the average of the other channels. We show in Figure 12, akin to Figures 8 and 9, the result of the denoising process for some fixed samples and various steps of the reward training, for the experiment with the most extreme incentive towards the reward. The objectives are reported for several experiments in Figure 13, for various values of the learning rate η and of the objective hyperparameter β .

We observe as for MNIST some mode collapse, although less pronounced here. Since the pretrained model has been trained with label conditioning for CIFAR-10, it is possible that this phenomenon could be a byproduct of this pretraining feature.

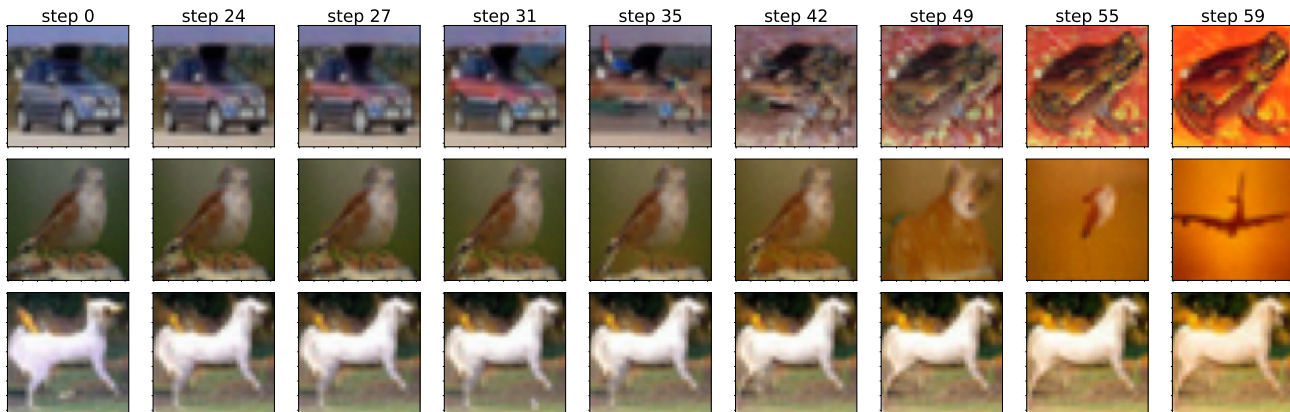


Figure 12. Reward training for a model pretrained on CIFAR-10. The reward incentives for **redder** images ($\lambda > 0, \beta > 0$). Selected examples are shown coming from a single experiment with $\lambda/\beta = 1,000$. All digits are re-sampled at the same selected steps of the Implicit Diffusion algorithm, as explained in Appendix C.2.

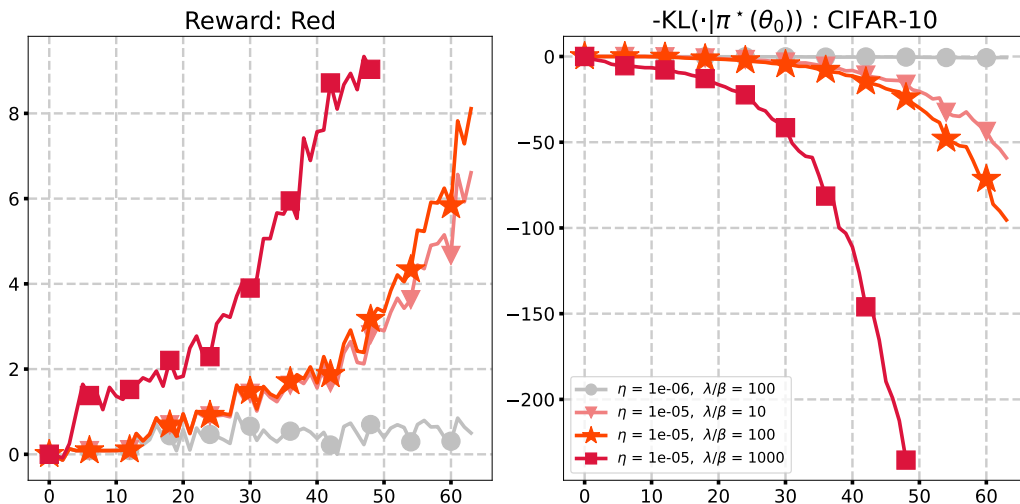


Figure 13. Score function reward training with **Implicit Diffusion** pretrained on CIFAR-10 for various $\lambda > 0$ (redder). **Left:** Reward, average brightness of image. **Right:** Divergence w.r.t. the original pretrained distribution.

D. Additional related work

Reward finetuning of denoising diffusion models. A large body of work has recently tackled the task of finetuning denoising diffusion models, with various point of views. [Wu et al. \(2023\)](#) update weight parameters in a supervised fashion by building a high-reward dataset, then using score matching. Other papers use reinforcement learning approaches to finetune the parameters of the model ([Dvijotham et al., 2023](#); [Fan et al., 2023](#); [Black et al., 2024](#)). Closer to our approach are works that propose finetuning of denoising diffusion models by backpropagating through sampling ([Watson et al., 2022](#); [Dong et al., 2023](#); [Wallace et al., 2023](#); [Clark et al., 2024](#)). However, they sample only once ([Lee et al., 2023](#)), or use a nested loop approach (described in Section 3.1) and resort to implementation techniques such as gradient checkpointing or gradient rematerialization to limit the memory burden. We instead depart from this point of view and propose a **single-loop** approach. Furthermore, our approach is much more general than denoising diffusion models and includes any iterative sampling algorithm such as Langevin sampling.

Single-loop approaches for bilevel optimization. Our single-loop approach for differentiating through sampling processes is inspired by recently-proposed single-loop approaches for bilevel optimization problems ([Guo et al., 2021](#); [Yang et al., 2021](#); [Chen et al., 2022](#); [Dagr  ou et al., 2022](#); [Hong et al., 2023](#)). Closest to our setting is [Dagr  ou et al. \(2022\)](#), where strong convexity assumptions are made on the inner problem while gradients for the outer problem are assumed to be Lipschitz and bounded. They also show convergence of the average of the objective gradients, akin to our Theorem 4.7. However, contrarily to their analysis, we study the case where the inner problem is a sampling problem (or infinite-dimensional optimization problem). Our methodology also extends to the non-stationary case, e.g. encompassing denoising diffusion models.

Study of optimization through Langevin dynamics in the linear case. In the case where the operator Γ can be written as an expectation w.r.t. p_t then the dynamics (12) can be seen as McKean-Vlasov process. [Kuntz et al. \(2023\)](#) propose efficient algorithms to approximate this process using the convergence of interacting particle systems to McKean-Vlasov process when the number of particles is large. In the same setting, where Γ can be written as an expectation w.r.t. p_t , discretization of such dynamics have been extensively studied ([Atchad   et al., 2017](#); [De Bortoli et al., 2021](#); [Xiao & Zhang, 2014](#); [Rosasco et al., 2020](#); [Nitanda, 2014](#); [Tadi   & Doucet, 2017](#)). In that setting, one can leverage convergence results of the Langevin algorithm under mild assumption such as [Eberle \(2016\)](#) to prove the convergence of a sequence $(\theta_k)_{k \in \mathbb{N}}$ to a local minimizer such that $\nabla \ell(\theta^*) = 0$, see [De Bortoli et al. \(2021, Appendix B\)](#) for instance.